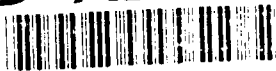


AD-A238 803



1



DTIC
ELECTE
JUL 23 1991
S D D

CALCULATED POINT DEFECT PROPERTIES OF
THE INTERMETALLIC COMPOUNDS
NICKEL TITANIUM (NiTi) and
IRON TITANIUM (FeTi)

THESIS

Russell T. Lutton, Captain, USAF

AFIT/GNE/ENP/91M-5

DISTRIBUTION STATEMENT A

Approved for public release;
Distribution Unlimited

DEPARTMENT OF THE AIR FORCE
AIR UNIVERSITY
AIR FORCE INSTITUTE OF TECHNOLOGY

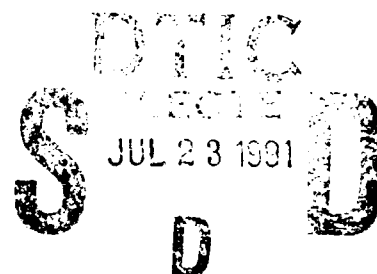
Wright-Patterson Air Force Base, Ohio

91 7 19 158

91-05720



AFIT/GNE/ENP/91M-5



CALCULATED POINT DEFECT PROPERTIES OF
THE INTERMETALLIC COMPOUNDS
NICKEL TITANIUM (NiTi) and
IRON TITANIUM (FeTi)

THESIS

Russell T. Lutton, Captain, USAF

AFIT/GNE/ENP/91M-5

91-05720



Approved for public release; distribution unlimited

91 01 2 16

AFIT/GNE/ENP/91M-5

CALCULATED POINT DEFECT PROPERTIES OF THE INTERMETALLIC
COMPOUNDS NICKEL TITANIUM (NiTi) AND IRON TITANIUM (FeTi)

THESIS

Presented to the Faculty of the School of Engineering
of the Air Force Institute of Technology
Air University

In Partial Fulfillment of the
Requirements for the Degree of
Master of Science in Nuclear Science

Russell T. Lutton, B.S., M.S.
Captain, USAF

March 1991

Approved for public release; distribution unlimited

Acknowledgments

The rewards of this thesis are received by me, but much of the burden of this assignment has been on by my wife, Maggie, and our daughter, Amanda. It is to them, I owe much more than thanks and give my love. My thanks to my faculty advisor Capt Sabochick, whose direction, help, understanding, and inspiration was excellent. I owe a special thanks to my classmates Mike Oehrli, Randy Wharton, and Chuck Wood for their help and support on this thesis.

NAME	DATE
CLASS	PERIOD
TEACHER	
STUDENT NO.	
BY	
DATE	
REMARKS	
DATE	APPROVED BY
	Signed
A-1	

Table of Contents

	Page
Acknowledgments	ii
List of Figures	iv
List of Tables	vi
Abstract	vii
I. Introduction	1
Background	1
Problem	3
Scope	3
Approach	4
II. Simulation Method	5
III. Antisite Defect	11
IV. Vacancy Defect Configuration and Migration ...	15
Ti Vacancy Defect Properties	15
Ni and Fe Vacancy Defect Properties	18
V. Vacancy Defect Formation Energy	23
VI. Interstitial Defect Configuration	30
Ti Interstitial Defect Properties	31
Ni and Fe Interstitial Defect Properties .	34
VII. Discussion	35
VIII. Conclusion	40
APPENDIX A: Code Description and Sample Files	44
APPENDIX B: Calculation Spreadsheet Results	49
APPENDIX C: Vacancy Formation Energy Code	56
APPENDIX D: Stable Defect Configuration Plots	69
Index	93
Bibliography	95
Vita	97

List of Figures

Figure	Page
1. B2-type Structure of FeTi and NiTi	7
2. Perfect Lattice Structure Cube for NiTi and FeTi .	11
3. Antisite Defect Lattice Structure for NiTi and FeTi	12
4. Ti Vacancy Stable Configuration with Ni or Fe Migration	16
5. Migration Energy Barriers for Ni-Fe Atoms to Ti Vacancy	17
6. Ni and Fe Vacancy Six-Jump Migration Sequence	20
7. Fe and Ni Vacancy Six-Jump Migration Graphic Results	21
8. Arrhenius plot of Vacancy Concentration vs. Temperature	29
9. Ti Interstitial Configuration for NiTi	32
10. Ti Interstitial Configuration for FeTi	32
11. Ni or Fe Interstitial Configuration for NiTi and FeTi	34
12. NiTi Lattice with Ti Vacancy Minimized	70
13. NiTi Lattice with Ti Vacancy Configuration	71
14. FeTi Lattice with Ti Vacancy Minimized	72
15. FeTi Lattice with Ti Vacancy Configuration	73
16. NiTi Lattice with Ni Vacancy Configuration	74
17. FeTi Lattice with Fe Vacancy Configuration	75
18. FeTi Lattice with Fe Vacancy Direct Migration Atom #569	76
19. FeTi Lattice with Fe Vacancy Migration Sequence 1 .	77
20. FeTi Lattice with Fe Vacancy Migration Sequence 4 .	78

Figure	Page
21. FeTi Lattice with Fe Vacancy Migration Sequence 5 .	79
22. FeTi Lattice with Fe Vacancy Migration Sequence 6 .	80
23. NiTi Ti Interstitial Configuration	81
24. NiTi Ti Interstitial Configuration <100> View	82
25. NiTi Ti Interstitial Configuration <010> View	83
26. NiTi Ti Interstitial Configuration <001> View	83
27. FeTi Ti Interstitial Configuration	84
28. FeTi Ti Interstitial Configuration <100> View	85
29. FeTi Ti Interstitial Configuration <010> View	86
30. FeTi Ti Interstitial Configuration <001> View	86
31. NiTi Ni Interstitial Configuration	87
32. NiTi Ni Interstitial Configuration <100> View	88
33. NiTi Ni Interstitial Configuration <010> View	89
34. NiTi Ni Interstitial Configuration <001> View	89
35. FeTi Fe Interstitial Configuration	90
36. FeTi Fe Interstitial Configuration <100> View	91
37. FeTi Fe Interstitial Configuration <010> View	92
38. FeTi Fe Interstitial Configuration <001> View	92

List of Tables

Table	Page
1. Antisite Defect Properties of NiTi and FeTi	14
2. Ni and Fe Antisite Defect Binding Energies	18
3. Antisite Defect Properties of NiTi and FeTi	19
4. Ni and Fe Vacancy Migration Energies	22
5. Interstitial Defect Properties	33
6. Stable Defect Configuration Energies ($E=U-U_0$)	36
7. Calculated Point Defect Energies (in eV)	37
8. FeTi "Ti" Vacancy Migration Data	50
9. NiTi "Ti" Vacancy Migration Data	50
10. FeTi "Fe" Vacancy Migration Data	51
11. NiTi "Ni" Vacancy Migration Data	53
12. Energies of the Most Stable Defect Configurations .	55
13. Vacancy Concentration of NiTi	63
14. Vacancy Concentration of FeTi	64
15. Vacancy Concentration of CuTi	65
16. Vacancy Concentration of CuTi ₂	65
17. Vacancy Concentration of FeTi, NiTi, CuTi, and CuTi ₂	67
18. Vacancy Formation Energy of FeTi, NiTi, FeTi, and CuTi ₂	68

Abstract

Atomistic simulation with a modified version of the DYNAMO code was used to calculate the point defect properties of the B2-type intermetallic compounds NiTi and FeTi. The calculated energies are believed to be experimentally accurate to within ± 0.1 eV.

The antisite pair formation energies for the alloys were calculated to be 1.015 eV for NiTi and 0.726 eV for FeTi. The antisite defect and vacant Ni or Fe lattice sites were found to be weakly bound with a binding energy 0.094 eV for NiTi and 0.055 eV for FeTi.

The vacancy defect configurations in NiTi and FeTi were identical. Vacant Ni or Fe lattice sites were preferred and had energy values of 6.356 eV for NiTi and 5.899 eV for FeTi. The Ni and Fe vacancy migrations had energy barriers of 1.272 eV for NiTi and 1.737 eV for FeTi. Removing a Ti atom resulted in a neighboring antisite defect caused by migrating Ni or Fe atoms into the vacant Ti lattice site. These configurations had energy values of 7.024 eV for NiTi and 6.336 eV for FeTi. The vacancy defect formation energies were calculated to be 1.48 eV for NiTi and 1.07 eV for FeTi.

The interstitial defect configurations consisted of Ni-Ni or Fe-Fe split-interstitial dumbbells centered on a Ti site with one or two adjacent Ti antisite defects. Ti interstitials resulted in two adjacent Ti antisite defects with a $\langle 011 \rangle$ direction Fe-Fe dumbbell or a $\langle 111 \rangle$ direction Ni-Ni dumbbell. The Ti interstitial defect energies were -2.395 eV for NiTi and -1.558 eV for FeTi. Ni or Fe interstitials both resulted in a single adjacent Ti antisite defect with Ni-Ni or Fe-Fe dumbbells oriented in the $\langle 111 \rangle$ direction. The Ni or Fe interstitial defect energies were -2.602 eV for NiTi and -1.945 eV for FeTi.

CALCULATED POINT DEFECT PROPERTIES OF THE INTERMETALLIC COMPOUNDS NICKEL TITANIUM (NiTi) AND IRON TITANIUM (FeTi)

I. Introduction

Background

The study of point defects for several decades has been of interest due to the role defects play in determining the physical properties of crystalline solids. This is especially true in those defects controlling the transport of matter and the properties stemming from it (Crawford, 1972, 1). For example, atom vacancies in the lattice structure are accepted as the dominant mechanism for self-diffusion in metals (Agullo-Lopez, 1988, 196). A point defect can be defined as "a perturbation that moves as an entity and whose properties are always the same, independent of how it has been generated and where it is located in an otherwise perfect crystal" (Gruber, 1964, 38). Some of the first papers in the study of point defect properties were done in calculating the defect formation and migration energies by Huntington and Seitz in 1942 (Gruber, 1966, 21). Irradiation of solids with electrons, neutrons and heavy ions result in lattice point defects. Thus, experiments with

irradiated materials have been used in the study of point defect formation and the development of atomistic simulation models of point defects (Gruber, 1966, 21). Recently, theories in amorphization of materials have given rise to an interest in the point defect properties of materials that can be amorphized, such as NiTi and FeTi (Sabochick, 1990, in press).

Recent computer simulation studies of the ordered compound copper titanium (CuTi) metal have shown that the properties of point defects in alloys may be considerably different than those of their pure metal counterparts (Shoemaker, et al., 1990, in press). Interstitials in this compound were found to have complicated configurations containing one or more antisite defects (where an atom is on a lattice site, but is of the wrong type). The complicated configuration implies the interstitials may not be as mobile as they are in pure metals. These results are different from what is observed in pure metals and support recent studies of the amorphization of CuTi (Shoemaker, et al., 1990, in press). Computer simulation of amorphization indicates the presence of point defects is critical in FeTi lattices, but chemical disorder may be more important in NiTi (Sabochick and Lam, 1990, in press). A comparison of point defect properties between the two compounds may reveal the reason for this behavior.

Problem

The problem is lack of information on the point defect properties of the intermetallic compounds nickel titanium (NiTi) and iron titanium (FeTi). These compounds are important because they can be amorphized using electron radiation. In addition, because NiTi and FeTi have the same crystal structure, the differences in their defect properties will result only from the differences between the nickel and iron elements. Thus, the results can be directly compared for understanding the effect each element has on point defects.

Scope

The problem is limited to single atom point defects in the NiTi and FeTi compound lattices. Thus the interaction of the defects are ignored, and the theories dependent on small concentrations of defects can be used to explore the defect properties. Specifically, the vacancies and interstitials of each atom type in each compound lattice will be explored with atomistic simulation. This will result in a total of eight case studies: (1) iron vacancy, (2) iron interstitial, (3) titanium vacancy in FeTi, (4) titanium interstitial in FeTi, (5) nickel vacancy, (6) nickel interstitial, (7) titanium vacancy in NiTi, and (8) titanium interstitial in NiTi.

Approach

The point defect properties of the compounds FeTi and NiTi are studied with computer atomistic simulation techniques with a modified version of the DYNAMO code. The general approach of the work is to:

1. Identify the stable vacancy configuration,
2. Calculate the migration energy of the vacancy,
3. Identify the stable interstitial configuration, and
4. Attempt to calculate the migration energy of the interstitial

for each of the individual compounds NiTi and FeTi. Interstitial configuration migration of similar compounds have proven difficult to calculate with the atomistic simulation techniques used in this work. The stable interstitial configuration of NiTi and FeTi were accompanied by antisite defects (see interstitial results section V). Thus, migration of the interstitial was not pursued.

II. Simulation Method

A modified version of the DYNAMO code called "RUNDYN" (see Appendix A for details) was used in the atomistic simulation required for the calculations in this work. The simulation techniques included; (1) molecular statics for the energy migrations and minimizations, (2) molecular dynamics with simulated annealing for vacancy calculations, and (3) Monte Carlo atom switching for the interstitial calculations.

In molecular dynamics Newton's equations of motion for the atoms are solved. The second order differential equations are solved numerically and yield the position and velocity of each atom at discrete times for the duration of the simulation. With the position and velocity of the atoms the lattice properties such as temperature, pressure, and internal energy are calculated (Sabochick, 1990, in press). In molecular statics, the atomic positions are calculated and the total potential energy of the lattice is minimized. This is usually done with mathematical minimization techniques such as steepest descent and conjugate gradients. In the modified version of the DYNAMO code the Fletcher-Powell minimization method was used in all of the calculations of this work. A more detailed explanation, with regards to the RUNDYN code, of atomistic simu-

lation is discussed by M. J. Sabochick in his report entitled "Basic Primer on Atomistic Simulation." Additional discussion on atomistic simulation is found in J. M. Haile's report entitled "A Primer on the Computer Simulation of Atomic Fluids by Molecular Dynamics."

All of the calculations had cubic volumes with periodic boundary conditions having fixed edge lengths and constant pressure. The embedded atom method (EAM) was used with the interatomic potentials derived with the method of Oh and Johnson (Shoemaker, et al., 1990, in press). The interatomic potential is used to specify the energy between atoms as a function of distance. These potentials were also used in the amorphization studies of NiTi and FeTi by M. J. Sabochick. The potentials for Ni, Fe, and Ti were fitted to the binding energies, lattice constants, elastic constants and vacancy formation energy of the pure metals (Shoemaker, et al., 1990, in press). The potentials for FeTi and NiTi were then determined by fitting the structure, lattice constants and heat of formation of the two compounds. The fitting procedure details have been described by Sabochick and Lam in other works (Sabochick and Lam, 1990, 565). The interatomic potential functions thus become the foundation for the point defect properties calculated in this work.

The potentials used give lattice parameters for FeTi as 2.976 ± 0.005 Angstroms ($\text{\AA} = 10^{-10}$ meters) and for NiTi as 2.998 ± 0.005 \AA . Both of these values are slightly larger than experimental values given by Duwey and Taylor as 2.975 ± 0.005 \AA for FeTi and 2.986 ± 0.005 \AA for NiTi (McQuillan, 1956, 221 and 239). These compounds both have body B2-type structures described as two interpenetrating equal sized cubic lattices shown in Figure 1 (Ghatak, 1972, 211). Each cubic lattice is of a different atom type with the corner atom of the opposite type at each cube's center position. Thus, in this simple lattice arrangement there is a total of 16 atoms with eight atoms of each type.

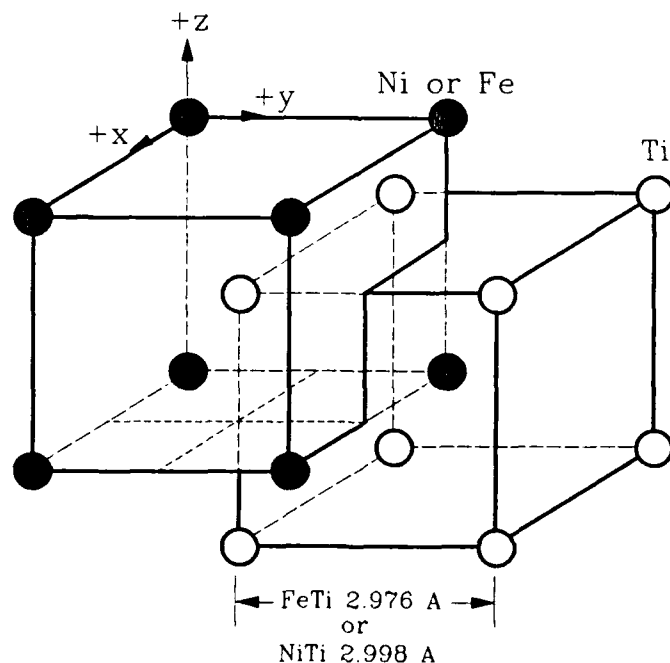


Figure 1. B2-type Structure of FeTi and NiTi

Point defects (especially interstitials) have many metastable energy configurations that require a technique to determine the global minimum energy (lowest energy, most stable) configuration (Shoemaker, et al., 1990, in press). First, a lattice structure of 1024 atoms was created with the RUNDYN code for both NiTi and FeTi. The stable and interstitial global minimum energy configurations were then determined with "simulated annealing" or "Monte Carlo atom switching" computer techniques. In the molecular dynamic "simulated annealing technique," a single atom was either removed (vacancy) or added (interstitial) at or near the center of the lattice and the energy of the lattice was minimized. These vacancy and interstitial lattices were then heated to 800 degrees Kelvin (K) and minimized to the lowest energy configuration using the Fletcher-Powell method (Shoemaker, et al., 1990, in press). After which, the lattice for each case was cooled in 50 or 100 degree increments to about room temperature at 300° K. The lowest energy configuration (global minimum) of these calculations was selected for each case from each group of calculations. Simulated annealing was adequate in finding the lowest energy configuration of vacancy point defects. However, for interstitial point defects calculations the Monte Carlo atom switching technique proved more efficient.

In the "Monte Carlo switching technique," atoms at a

constant temperature were randomly switched from one type to another creating antisite defects (where an atom is on a lattice site, but is of the wrong type). The total number of each type of atom is conserved in the switching and the lowest energy configuration is found after the atoms are switched. This technique is relatively new for use with the RUNDYN code (Shoemaker, et al., 1990, in press) and was found to reduce computational time and to be more efficient in calculating the interstitial configurations. Both the annealing and switching techniques were used in searching for the interstitial global minimum energy configurations (most stable). However, the final configurations were usually found with a little additional deductive reasoning to the calculated configurations.

After finding the lowest energy configuration or global minimum the results of the vacancy calculations were explored to find the required energy for individual atoms to migrate between lattice sites. Migration energies were calculated by minimizing the lattice energy as a jumping atom (the atom moving between lattice sites) was constrained at various distances from a vacancy in the lattice (see Appendix A for details). These calculations provided the required energy for atoms to move within the lattice and thereby overcome migration energy barriers.

Error assessment is not generally discussed in most atomistic simulation works. Haile makes note of it in his report concerning the numerical solution of Newton's equations. He notes that, errors are "primarily due to (a) use of a finite-difference algorithm for solving differential equations and (b) round-off errors that occur in the computer hardware" (Haile, 1980, 38). In all of the calculations with RUNDYN seven digits after the decimal point are repeatable if the tolerance was set at $1.0 \text{ E-}13$ (see Appendix B). The results are thus precise but without direct experiment results may lack accuracy. Enough past work has been done with the DYNAMO code that the accuracy of the work is believed to be within a few tenths (± 0.1 eV) of an eV (Sabochick, Dec 1990, personal discussion). The results here are presented with 3 or 4 significant digits, which is generally adequate for comparing results.

The antisite defect (where an atom is on a lattice site, but is of the wrong type) is the simplest defect of an ordered compound such as NiTi or FeTi (Figure 3).

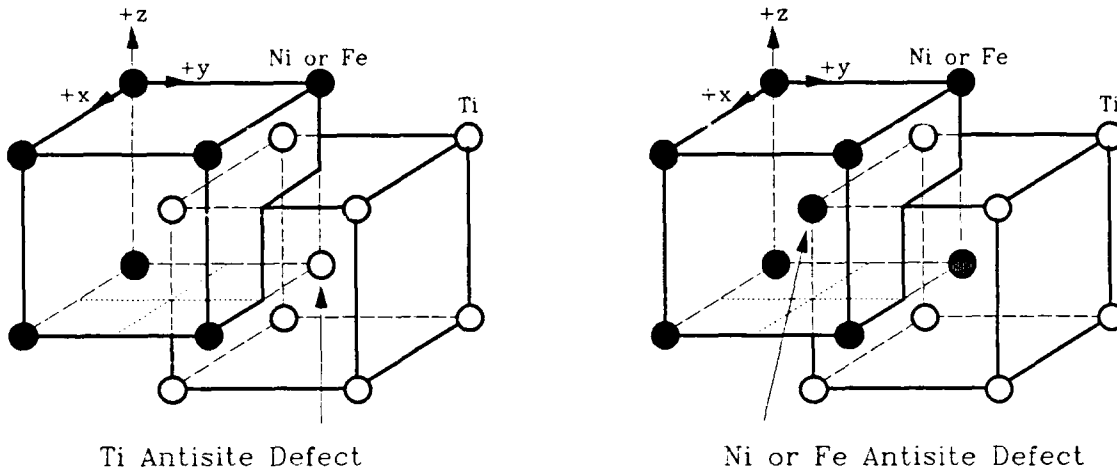


Figure 3. Antisite Defect Lattice Structure for NiTi and FeTi

The formation energy of the antisite defect pair is easily calculated with the RUNDYN code system lattice results. First, a single atom in the perfect lattice is converted to the opposite type atom (Figure 3) and a minimization calculation is performed on the resulting lattice. Second, this is done for each atom type in the compound lattice and the perfect lattice energy (U_0) is subtracted from each of the antisite defect lattice energies (U_a^{Ni} and U_a^{Ti} ; U_a^{Fe} and U_a^{Ti}). For example, in the NiTi lattice the equations for the individual antisite defect energies (E_a^{Ni} and E_a^{Ti}) are:

III. Antisite Defect

The perfect lattice structure used in all the calculations was a cube consisting of repeating interpenetrating simple cubic structures (Figure 1) with 8 atoms to a side having side dimensions of 11.992 Angstroms(\AA) for NiTi and 11.904 \AA for FeTi (Figure 2). The total energy (U_0) of the perfect lattice containing 1024 lattice sites (N_S) was $U_0^{\text{Ni}} = -5120.861$ eV for the NiTi lattice and was $U_0^{\text{Fe}} = -5008.453$ eV for the FeTi lattice.

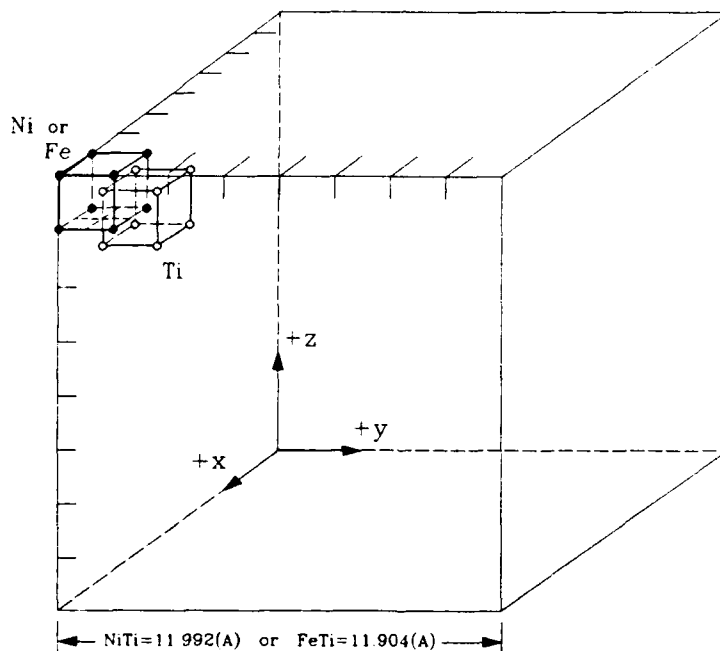


Figure 2. Perfect Lattice Structure used for NiTi and FeTi

$$E_a^{Ni} = U_a^{Ni} - U_o \quad (1)$$

$$E_a^{Ti} = U_a^{Ti} - U_o \quad (2)$$

Finally, the Ni antisite pair formation energy E_f^{Ni} is calculated by adding the individual antisite defect energies E_a^{Ni} and E_a^{Ti} .

$$E_f^{Ni} = E_a^{Ni} + E_a^{Ti} \quad (3)$$

The equations (1), (2), and (3) are identical for the FeTi alloy with the Ni superscript exchanged with a Fe. The antisite pair formation energies for both alloys were calculated from the code results given in Table 1 as 1.015 eV for NiTi and 0.726 eV for FeTi. In creating the antisite defects the energy increase was larger (less negative) when converting Ti atoms to either nickel (Ni) or iron (Fe) than when converting Ni or Fe to Ti (Table 1). This implies that Ni or Fe antisite defects should be preferred over Ti antisite defects in the lattice. A Ti vacancy in the lattice would therefore have a higher potential of being filled with a Ni or Fe atom and thereby create a Ni or Fe antisite defect. The stable vacancy configurations given in the next section confirm this observation.

Table 1. Antisite Defect Properties ($E_x^y = U_x^y - U_o$)					
		NiTi (y=Ti)		FeTi (y=Fe)	
System	x y	$U_x^y(\text{eV})$	$E_x^y(\text{eV})$	$U_x^y(\text{eV})$	$E_x^y(\text{eV})$
Perfect Crystal	o	-5120.861	0.0	-5008.453	0.0
Ni or Fe Antisite	a y	-5120.098	0.762	-5007.962	0.491
Ti Antisite	a Ti	-5120.608	0.253	-5008.218	0.235
			$E f_x^y$		$E f_x^y$
Antisite Formation	a y		1.015		0.726

If experimentally neither of these compounds becomes chemically disordered when heated, it would imply that the antisite defect pair formation energy is significantly larger than the Boltzmann's constant (k) multiplied by the melting temperature (T_m) of the given alloy (Shoemaker, et al., 1990, in press). The melting temperatures of NiTi and FeTi are 1615° K and 1590° K respectively (McQuillan, 1956, 236 and 217). Thus, given the value of $k = 8.61735\text{E-}5 \text{ eV/K}$ then the value of $k \cdot T_m$ is equal to 0.139 eV and 0.137 eV for NiTi and FeTi respectively. These alloys should not become chemically disordered when heated, because the antisite formation energies are significantly larger (1.015 eV for NiTi and 0.726 eV for FeTi) than their respective $k \cdot T_m$ values.

IV. Vacancy Defect Configuration and Migration

Ti Vacancy Defect Properties

A single Ti atom was removed from the center of the perfect lattice and placed at the end of the restart file for both NiTi and FeTi. This allowed the atoms to be renumbered for easily tracking the movement of surrounding atoms. This same Ti atom #1024 was then permanently removed from the lattice and a Ti vacancy was created. Using the simulated annealing technique, the resulting minimum lattice energy of these Ti vacancy lattices was -5113.8369 eV and -5002.1175 eV for NiTi and FeTi respectively. The stable Ti vacancy configurations had higher energy levels than the perfect lattice by 7.0238 eV for NiTi and 6.3355 eV for FeTi (Table 3). Stability of these configurations was achieved by the migration of an adjacent Ni or Fe atom into the Ti vacancy (Part A in Figure 4). The resulting configuration in both compounds consisted of a vacant Ni or Fe site and an adjacent Ni or Fe antisite defect (Part B in Figure 4).

The migration energy barriers to the migrating Ni or Fe atoms were calculated with the molecular statics technique described in the simulation section. The Ni or Fe atom migration energy barriers were calculated to be 0.1344 eV for NiTi and 0.3407 eV for FeTi.

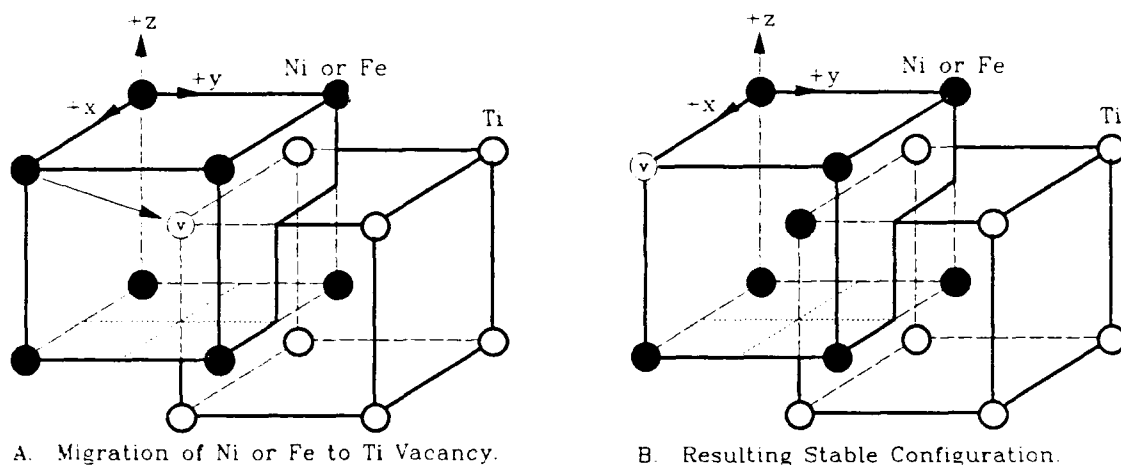


Figure 4. Ti Vacancy Stable Configuration with Ni or Fe Migration

Each of these migrations is shown graphically in Figure 5 for equally spaced stepped migration distances. See Appendix A for a description of the migration method and Appendix B for tabulated migration results. In the final stable configuration the adjacent atoms around the vacancy were displaced slightly towards the vacancy. This relaxation around the vacancy did not cause large displacements of the atoms off their normal lattice sites for NiTi nor for FeTi (see Appendix D for computer output plots).

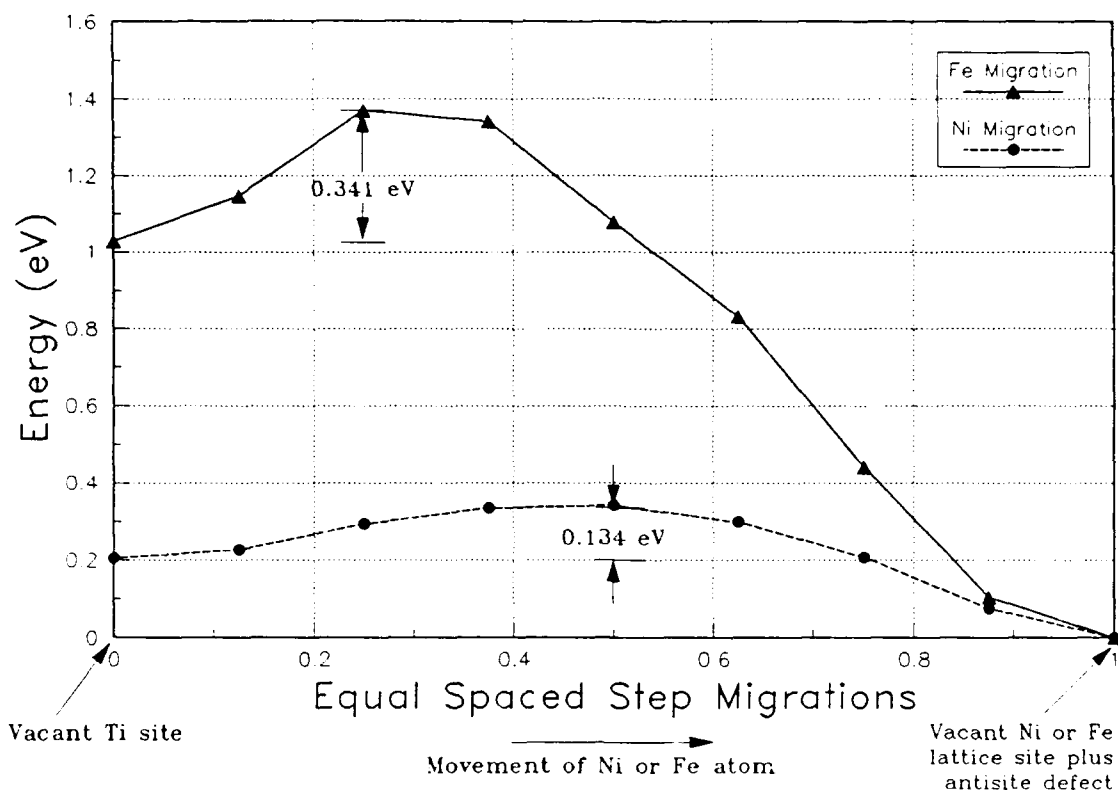


Figure 5. Migration Energy Barriers for Ni or Fe Atoms to Ti Vacancy

The Ni or Fe antisite defect binding energies to a Ti vacancy were calculated using the results of the vacancy defect calculations given in Table 3 and the antisite defect results given in Table 1. This binding energy is the energy required to remove the Ni or Fe antisite defect from the lattice and replacing the resulting vacancy with a Ti atom. This was done by adding the Ni or Fe vacancy energies to the Ni or Fe antisite defect energies for their individual alloy types (Table 2). The Ti vacancy energies were then subtracted from the above results for their

respective compounds. This resulted in the binding energies for each of the compounds (Table 2). The antisite defect and vacant Ni or Fe sites were found to be weakly bound with a binding energy of 0.094 eV for NiTi and 0.055 eV for FeTi.

Table 2. Ni and Fe Antisite Defect Binding Energies				
System	Number of Atoms		Energy (eV)	
	Ni or Fe	Ti	NiTi	FeTi
A. Perfect Crystal	512	512	0.0	0.0
B. Ti Vacancy	512	511	7.0238	6.3355
C. Sum = A + B	1024	1023	7.0238	6.3355
D. Ni or Fe Antisite	513	511	0.7623	0.4910
E. Ni or Fe Vacancy	511	512	6.3558	5.8993
F. Sum = D + E	1024	1023	7.1181	6.3903
Binding Energy = F - C			0.0943	0.0548

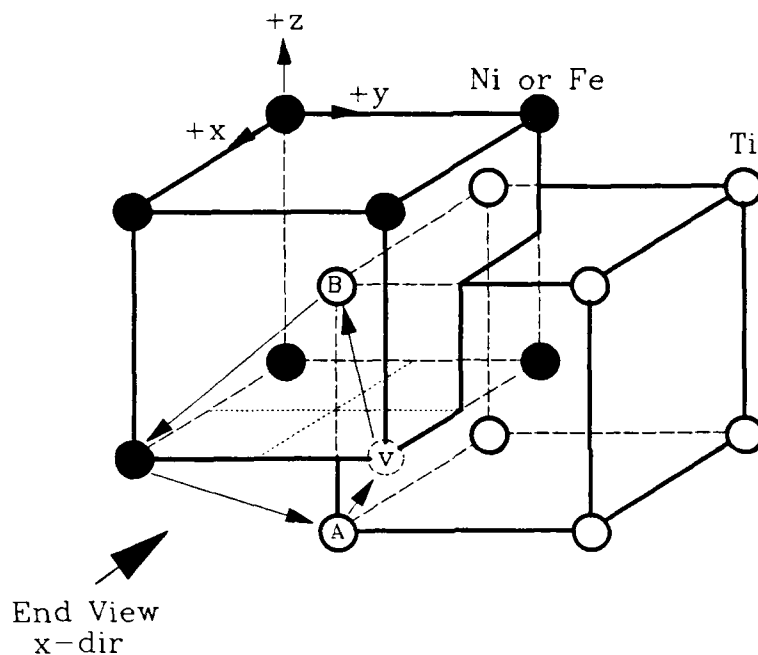
Ni and Fe Vacancy Defect Properties

The Ni or Fe vacancy lattices were created in the same way as the initial Ti vacancy lattices. The resulting relaxation of the adjacent atoms surrounding the vacancy proved to be the lowest energy configuration, as no readjustment of the lattice resulted from the applied simulated annealing technique. Thus, the stable configuration of a vacancy after removal of a Ni atom was a vacant Ni site for both compounds. The resulting calculated lattice energy

values are given in Table 3.

Table 3. Vacancy Defect Properties of NiTi and FeTi($E_x^v = U_x^v - U_o$)					
		NiTi (y=Ni)		FeTi (y=Fe)	
System	x y	$U_x^v(\text{eV})$	$E_x^v(\text{eV})$	$U_x^v(\text{eV})$	$E_x^v(\text{eV})$
Perfect Crystal	o	-5120.861	0.0	-5008.453	0.0
Ni or Fe Vacancy	v y	-5114.505	6.356	-5002.554	5.899
Ti Vacancy	v Ti	-5113.837	7.024	-5002.118	6.336

The migration barrier calculation of either the Ni or Fe vacancy consists of a six-jump ring sequence. The vacant Ni or Fe site is rotated through its nearest neighbors (atoms A and B in Figure 6) to the next Ni or Fe lattice site. The migration energy barriers calculated through this sequence were 1.2718 eV and 1.7382 eV for NiTi and FeTi respectively. These migration values are relatively large compared to typical vacancy migration energies in pure metals. This can be attributed to the intermediate configurations containing antisite defects and or vacant Ti site (Sabochnik, 1990).



Migration Sequence

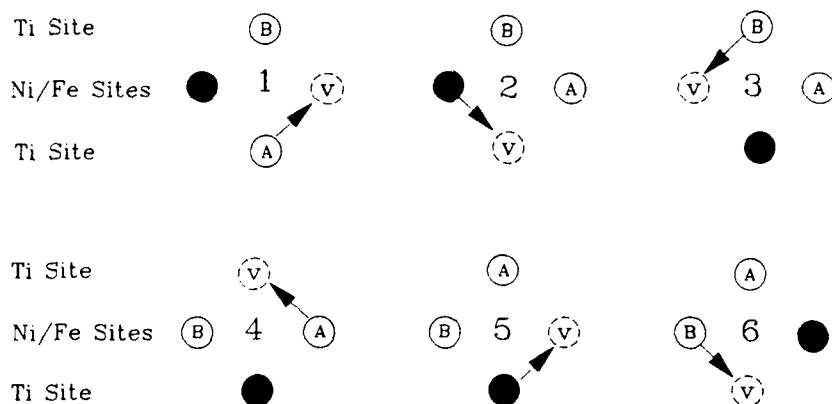


Figure 6. Ni and Fe Vacancy Six-Jump Migration Sequence

The migration sequence is shown graphically in Figure 7 and the individual migration energies are given in Table 4.

Both the Ni and Fe migration sequences are similar except the energy barrier occurs in the second and fifth steps of the sequence for the FeTi lattice verses the third and

forth steps for the NiTi lattice (Figure 7). In the FeTi lattice the first migration sequence also results in an unstable (no metastable) configuration.

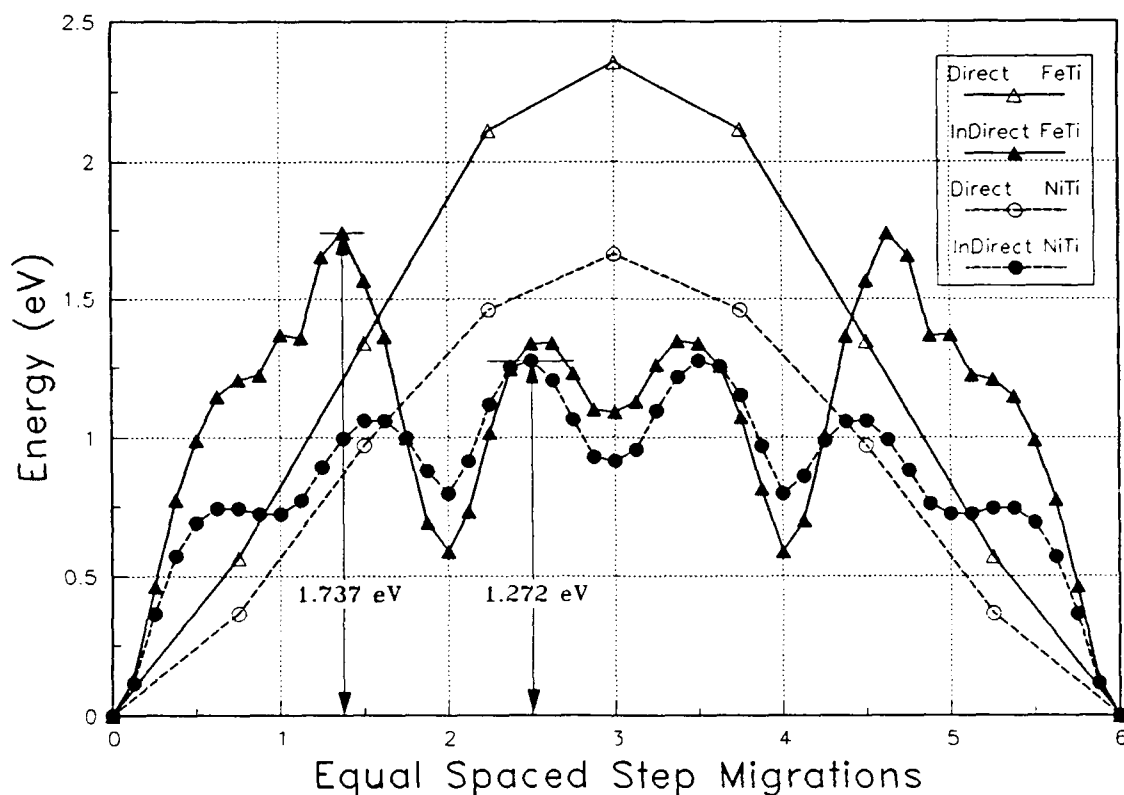


Figure 7. Fe and Ni Vacancy Six-Jump Migration Graphic Results

The direct migration of the vacancy to its second nearest neighbor location was also calculated for comparison to the nearest neighbor (indirect) migration. These direct migration values 1.6594 eV for NiTi and 2.3556 eV for FeTi were significantly higher than the ring sequence migration sequence for both compounds (Figure 7 and Table 4).

Table 4. Ni and Fe Vacancy Migration Energies		
Migration Path	X=Ni (eV)	X=Fe (eV)
Ti to X Vacancy	0.366	1.206 (c)
X to Ti Vacancy (a)	1.057	1.738
Ti to X Vacancy (b)	1.272	1.339
Direct Migration		
X to X Vacancy	1.659	2.356
(a) with 1 adjacent antisite defect. (b) with 2 adjacent antisite defects. (c) unstable configuration.		

V. Vacancy Defect Formation Energy

Experiments with solids in which point defects were observed has given information about the energies of defect formation, volume changes, and binding energies of the defects. From this information the theory of atomistic models of defects has developed. The theory is used in atomistic simulation (1) to determine the configuration of atoms for certain (antisite, vacancy, or interstitial) defects in a given material and (2) to calculate the values of these quantities (Gruber, 1966, 21).

Experimental quenching techniques have been used in conjunction with direct observation by ion microscopy to determine the energy of vacancy defect formation. For example, in one such experiment (Newkirk and Wernick, 1962, 84) a platinum tip was quenched from a temperature (T) of 1800° K and five vacancies (N_{vac}) were found by ion microscopic inspection. The total number of atoms (N) of the inspected material was 8500 and the vacancy concentration ($C_v = N_{vac}/N$) is equal to $5.9E-4$ by direct counting. Assuming this concentration was frozen in the platinum by the quenching and assuming the vacancies were in thermal equilibrium, the energy of formation is ($E_f = kT \ln(C_v)$) equal to 1.15 eV, where $k = 8.61735E-5$ (eV/K) is the Boltzmann constant. This technique works well with pure

metals but is complicated by the presence of other atom types, as in alloys. Computational simulation techniques can however be used determine the formation energies in alloys.

In pure metals, the vacancy is of only one type of atom without the possibility of antisite defects. The formation energy is calculated from the potential energy of the perfect lattice and the energy of the lattice with the vacancy defect. In impure metals and alloys a more complex variety of point defects is present, these include antisite defects and vacancies of each type of atom in the alloy. The calculation of the formation energy is dependent on knowing the potential energies of each of these point defects. One method of determining the vacancy formation energy is to calculate the concentration of the defect (C_v) as a function of temperature (T) where the defect energy of formation (E_f) is given by

$$E_f(T) = -k \frac{d[\ln(C_v)]}{d[T^{-1}]} \quad (4)$$

The concentration of the vacancy defect (C_v) as a function of temperature was calculated using the method by Foiles and Daw (Foiles and Daw, 1987, 12-13). In this method, the concentrations of the defects are assumed small such that the defects can be treated as noninteracting.

For the NiTi alloy, there is one Ni lattice site for each Ti site. Each lattice site can be occupied by either an atom appropriate to the sublattice, by a vacancy, or by an atom of the opposite type (e.g. antisite defect). In such a system for the NiTi lattice the total potential internal energy U is

$$U = U_o + N_s (n_v^{Ni} E_v^{Ni} + n_v^{Ti} E_v^{Ti} + n_a^{Ni} E_a^{Ni} + n_a^{Ti} E_a^{Ti}) \quad (5)$$

where U_o is the energy of the perfect lattice with N_s lattice sites, n_v^{Ni} , n_v^{Ti} , n_a^{Ni} , and n_a^{Ti} are the defect concentrations of Ni vacancies, Ti vacancies, Ni antisite defects, and Ti antisite defects respectively. In this system the total concentration of the vacancies is equal to the sum of the individual vacancies of each type of atom ($C_v = n_v^{Ni} + n_v^{Ti}$). The corresponding energies E_v^{Ni} , E_v^{Ti} , E_a^{Ni} , and E_a^{Ti} are the differences in energy between the system containing a single defect and the perfect lattice (e.g. $E_v^{Ni} = U_v^{Ni} - U_o$). These energy values are presented for the antisite defects in Table 1 and for the vacancy defects in Table 3. The configuration entropy S of the system is

$$S = N_s \left\{ \frac{1}{2} [s(2n_v^{Ni}) + s(2n_a^{Ti})] + \frac{1}{2} [s(2n_v^{Ti}) + s(2n_a^{Ni})] \right\} \quad (6)$$

where s is the ideal entropy function.

$$s(x) = -[x \ln(x) + (1-x) \ln(1-x)] \quad (7)$$

The total number of Ni atoms (N^{Ni}), is given by

$$N^{Ni} = N_s \left(\frac{1}{2} - n_v^{Ni} + n_a^{Ni} - n_a^{Ti} \right) \quad (8)$$

and similarly for the total number of Ti atoms (N^{Ti}) in the configuration with the Ni and Ti superscripts exchanged. The antisite concentration was shown by Foiles and Daw to equal

$$n_a^{Ni} = \frac{1}{2} \left\{ \frac{\exp[-(E_a^{Ni} + \mu^{Ti} - \mu^{Ni})/kT]}{1 + \exp[-(E_a^{Ni} + \mu^{Ti} - \mu^{Ni})/kT]} \right\} \quad (9)$$

and for the vacancy concentration to equal

$$n_v^{Ni} = \frac{1}{2} \left\{ \frac{\exp[-(E_v^{Ni} + \mu^{Ni})/kT]}{1 + \exp[-(E_v^{Ni} + \mu^{Ni})/kT]} \right\} \quad (10)$$

where μ^{Ni} and μ^{Ti} are the chemical potentials of the respective atom types. The equations for n_a^{Ti} and n_v^{Ti} are identical with Ni and Ti superscripts exchanged for the respective atoms. The chemical potentials can be eliminated by using their relationship to the Gibb's free energy

$$U - kTS = \mu^{Ni} N^{Ni} + \mu^{Ti} N^{Ti} \quad (11)$$

U and substituting the total potential energy U given in equation (5) and the configuration entropy S given in equation (6). Requiring the total number of atoms at a given temperature to equal the stoichiometry of the compound

$$\frac{1}{2} = \frac{N^{Ni}}{N^{Ni} + N^{Ti}} \quad (12)$$

allows the eight unknowns N^{Ni} , N^{Ti} , n_a^{Ni} , n_v^{Ni} , n_a^{Ti} , n_v^{Ti} , μ^{Ni} , and μ^{Ti} to be solved by the eight equations (8a,8b), (9a,9b), (10a,10b), (11), (12), and their complements. All of these equations are the same for the FeTi alloy with the Ni subscripts exchanged with Fe and the appropriate Ti energy values used for FeTi. These equations were implemented into the TK Solver Plus software program to facilitate graphing and tabulating the results (Appendix C). The only required input values to the program are the five total system energies for the global minimum configurations and the number of lattice sites for each type of atom in the compound. These energies include the perfect crystal U_0 for each alloy, the antisite defect total

system energies for NiTi U_a^{Ni}, U_a^{Ti} or for FeTi U_a^{Fe}, U_a^{Ti} (Table 1), plus the vacancy defect total system energies for NiTi U_v^{Ni}, U_v^{Ti} or for FeTi U_v^{Fe}, U_v^{Ti} (Table 3).

The vacancy concentrations calculated with the above system of equations were used to calculate the vacancy formation energy of each compound. This was done by calculating the slope of the log of C_v vs $1/T$ shown in the Figure 8 Arrhenius plot. The vacancy formation energy is a function of temperature, however at lower temperatures (below about 1200° K) its dependence is negligible. The curves in Figure 8 are essentially straight indicating that a single formation energy value can be used over the entire temperature range. The effective vacancy formation energies were calculated to be 1.48 eV for NiTi and 1.07 eV for FeTi. These values compare reasonably well with the values of CuTi (1.09 eV) and CuTi₂ (0.90 eV), which were calculated with the same method from data given by Shoemaker's DYNAMO calculations (Shoemaker, et al., 1990, in press). No experimental values for the compounds were found, however these formation energies are generally lower than those of the individual pure metals. For example, the experimental formation energies of the metals Ni (1.7 +/- 0.1 eV, Agullo-Lopez et al., 1988, 1997) and Ti (1.55 +/- 0.1 eV, Shoemaker, et al., 1990, in press) are larger than those of the NiTi compound (1.48 +/- eV).

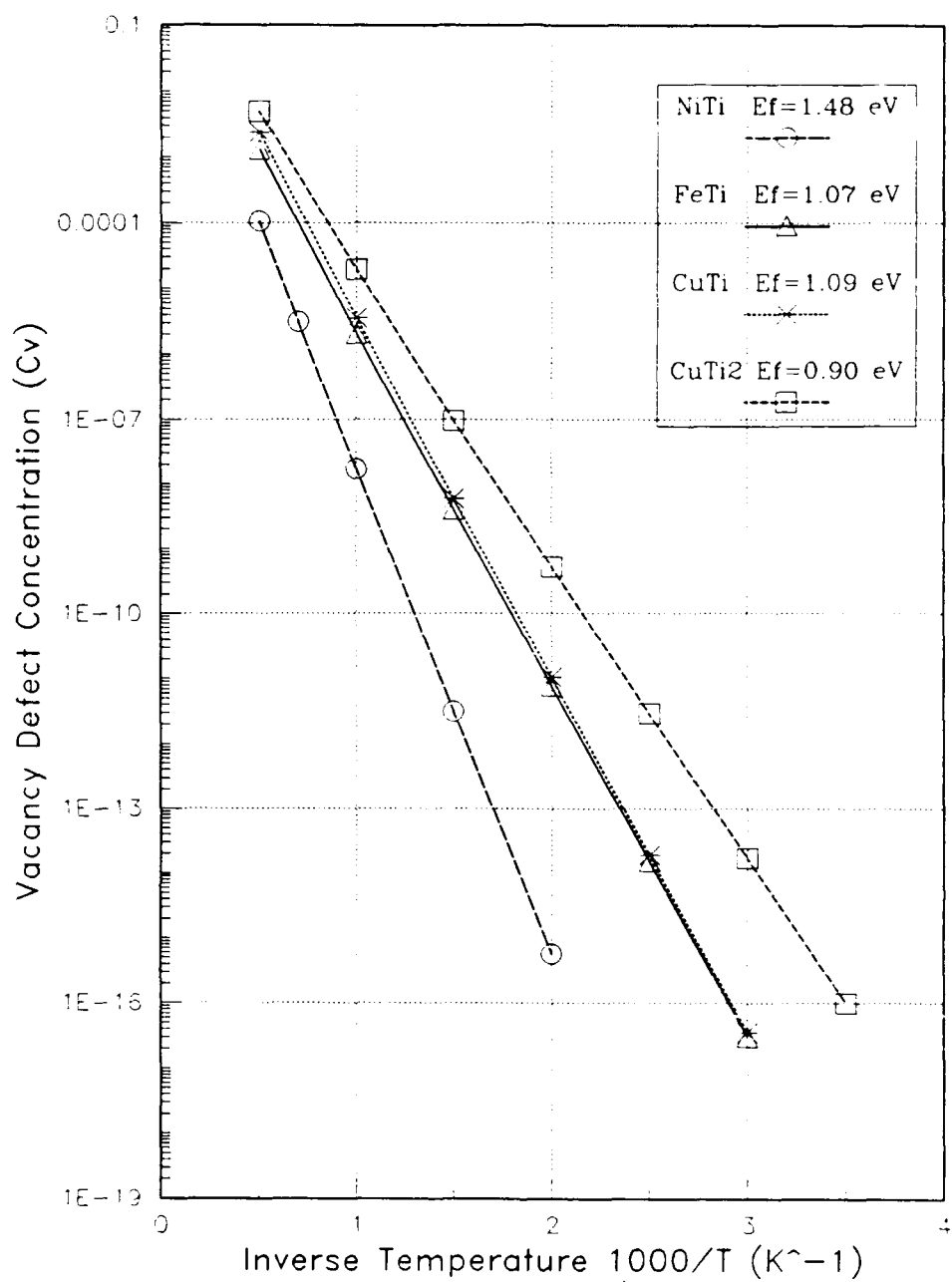


Figure 8. Arrhenius Plot of Vacancy Concentration vs. Temperature

VI. Interstitial Defect Configuration

The interstitial calculations had the same perfect lattice structure as the vacancy calculations. A single titanium (Ti) atom was added near the center of the lattice by placing it at the end of the restart file. This again allowed the atoms movement to be easily tracked by their atom numbers and avoided graphical viewing problems associated with the edge of the lattice. The resulting minimized lattice became the basis for all the other calculations.

The annealing simulation technique proved to be an ineffective method for finding the global minimum configuration. It appears the annealing technique did not allow the antisite defects to be formed easily. The Monte Carlo switching technique easily formed antisite defects and proved to be the most useful in determining the interstitial configuration. However, in all cases the final configuration was determined with a little added inductive reasoning based on the Monte Carlo calculation results. The Monte Carlo technique is dependent on finding a critical temperature to allow switching to occur in the lattice without overwhelming the process with too many antisite defect switches. For FeTi no switches occurred at 520 degrees K and too many occurred at 550 degrees K. Thus the

critical temperature used for FeTi was 530 K and for NiTi was 720 K. Once the critical temperature was established the calculation could be repeated with different random seed numbers, which should generate similar results. All of the interstitial configurations were generated in this same fashion.

Ti Interstitial Defect Properties

The final stable configuration consisted of a Ni-Ni or Fe-Fe dumbbell centered on a Ti site with 2 adjacent Ti antisite defects (Ti on Ni or Fe site) at opposite corners of the Ni or Fe cube (Figure 9 and 10). These configurations were the same for NiTi and FeTi except for the direction of the dumbbell. The Ni-Ni dumbbell (split-interstitial) was oriented in the $\langle 111 \rangle$ unit vector direction with relatively large displacements (off the lattice site) of the atoms along the $\langle 111 \rangle$ direction. Output plots of these configurations are given in Appendix D.

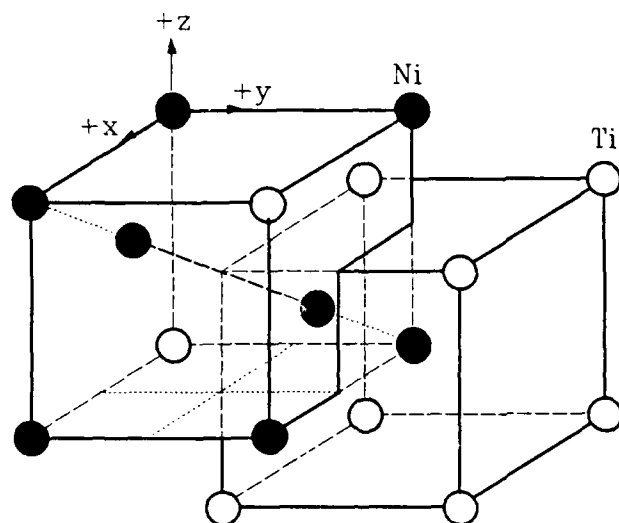


Figure 9. Ti Interstitial Stable Configuration for NiTi

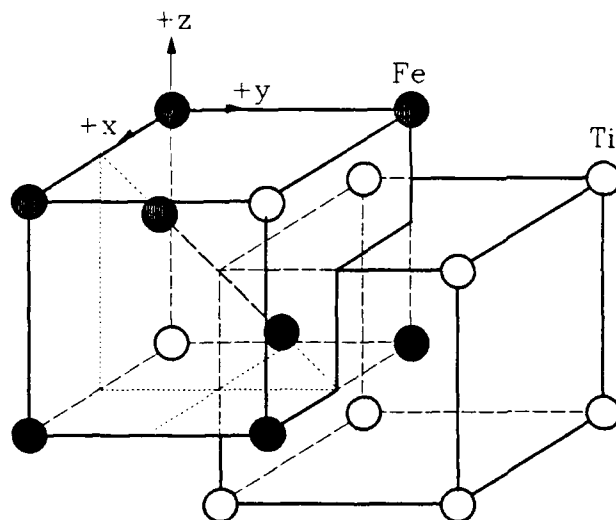


Figure 10. Ti Interstitial Stable Configuration for FeTi

No quantitative measurements of the displacements were made and the subjective terms large, small, or slight are relative to each other. RUNDYN code output plots of all of the configurations are given in Appendix D for comparison of displacements. The Fe-Fe dumbbell was oriented in the

<011> direction (Figure 10) with significant but smaller displacement of the neighboring atoms in the <011> direction. The values of the stable configuration energies and Frenkel pair formation energies are given in Table 4.

Table 5. Interstitial Defect Properties ($E_x^y = U_x^y - U_o$)					
		NiTi (y=Ni)		FeTi (y=Fe)	
System	x y	U_x^y (eV)	E_x^y (eV)	U_x^y (eV)	E_x^y (eV)
Perfect Crystal	o	-5120.861	0.0	-5008.453	0.0
Ni/Fe Interstitial	i y	-5123.256	-2.395	-5010.011	-1.558
Ti Interstitial	i Ti	-5123.463	-2.602	-5010.398	-1.945
Ni/Fe Frenkel Pair	f y		3.961		4.341
Ti Frenkel Pair	f Ti		4.422		4.391

Ni and Fe Interstitial Defect Properties

The Ni and Fe interstitial configurations were calculated in the same manor as the Ti interstitial. The resulting global minimum energy configurations (Figure 11) for both NiTi and FeTi consisted of a Ni-Ni or Fe-Fe dumbbell oriented in the $\langle 111 \rangle$ unit vector direction with an adjacent single Ti antisite defect (Ti on Ni or Fe site). The stable defect configuration energies and calculated point defect energies are given in Table 4 for all the interstitial defects.

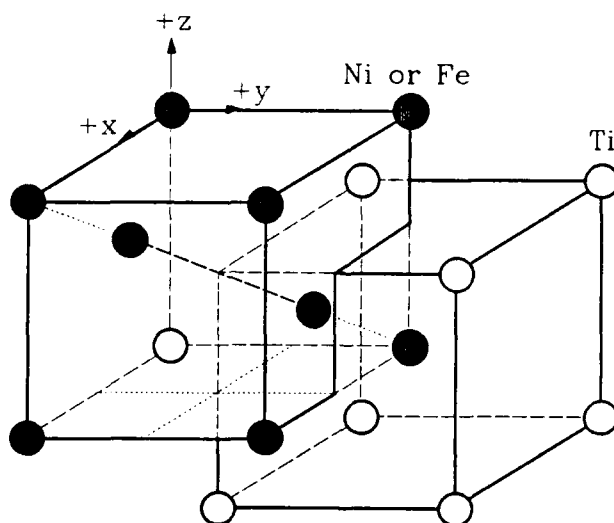


Figure 11. Ni or Fe Interstitial Configuration for NiTi and FeTi

VII. Discussion

The stable antisite defect configurations (Table 6) were calculated and used to determine the formation energies and binding energies (Table 7) for both NiTi and FeTi. The resulting NiTi antisite pair formation energy is over twice as that of the energy for either CuTi or CuTi₂. Sabochick and Lam explored the key factors for inducing the crystalline-to-amorphous (C-A) transition in NiTi. They concluded that point defects are necessary for amorphization to occur, but that chemical disorder was sufficient to store the energy necessary to make the transition (Sabochick and Lam, 1990, in press). The large energy necessary for NiTi antisite pair formation explains why chemical disordering can store large amounts of energy in NiTi. With the large FeTi antisite pair energy, one would expect similar amorphization behavior in FeTi as is found in the NiTi alloy.

The stable vacancy configurations of both NiTi and FeTi preferred Ni or Fe sites for vacancies in both the Ti vacancy and Ni/Fe vacancy calculations. The Ti vacancy was filled by a migrating Ni or Fe and resulted in a Ni or Fe antisite defect with a neighboring vacant Ni or Fe site.

This same site preference was noted to occur in both the CuTi and CuTi₂ compounds (Shoemaker, et al., 1990, in press).

Table 6. Stable Defect Configuration Energies ($E = U - U_0$)			
System	Number of Atoms	NiTi (eV)	FeTi (eV)
Ti Antisite (a)	1024	0.253	0.235
Ni or Fe Antisite (b)	1024	0.762	0.491
Ti Vacancy	1023	7.024	6.336
Ni or Fe Vacancy	1023	6.356	5.900
Ti Interstitial (c & d)	1025	-2.602	-1.945
Ni or Fe Interstitial (e)	1025	-2.395	-1.558
(a) Ti on Ni or Fe Lattice Site. (b) Ni or Fe on Ti Lattice Site. (c) NiTi <111> split-interstitial with two Ti antisite defects. (d) FeTi <011> split-interstitial with two Ti antisite defects. (e) Both <111> split-interstitials with one Ti antisite defect.			

It is well accepted that vacancy migration is the dominant mechanism for self-diffusion in metals (Agullo-Lopez and others, 1988, 1996). The vacancy migration energies (Table 7) for NiTi (1.27 eV) and FeTi (1.74 eV) are similar to those for CuTi (0.19/1.32 eV) and CuTi₂ (0.92). The higher FeTi energy indicates diffusion is more difficult in this alloy than either NiTi, CuTi, or CuTi₂. The higher vacancy migration energies may be explained by (1) the antisite defects formed in the migration sequence and by (2) the large antisite pair energies of NiTi and FeTi. The vacancy formation energy for FeTi (1.07 eV) is,

however, significantly lower than that of NiTi (1.48 eV). Thus, although vacancies are more easily formed in FeTi their migration is more difficult. Although no experimental vacancy formation energies were found for the alloys, these calculated values are lower than the experimental values for the pure metals of the compounds. For example for NiTi the pure metal values are 1.7 (+/- 0.1) eV for Ni (Agullo-Lopez and others, 1988, 197) and 1.55 eV for Ti (Shoemaker, et al., 1990, in press). This indicates the vacancy formation is easier in both alloys NiTi and FeTi than in their pure metals. The same results was noted by Shoemaker for CuTi and CuTi₂.

Table 7. Calculated Point Defect Energies (in eV)				
System	NiTi	FeTi	CuTi (a)	CuTi ₂ (a)
Antisite Pair Formation	1.015	0.726	0.385	0.460
Antisite Binding	0.094	0.055		
Vacancy Migration	1.272	1.738	0.19/1.32	0.92
Vacancy Formation	1.48	1.07	1.09	0.90
Frenkel Pair Ti Formation	4.422	4.391		
Frenkel Pair Ni, Fe, or Cu	3.961	4.341	2.769	2.776
Interstitial Formation (b)	2.5	3.3	1.7	1.9
(a) Shoemaker, et al., 1990, in press.				
(b) Estimated by subtracting the Vacancy Formation from the Frenkel Pair Energy.				

The interstitial configurations of both NiTi and FeTi were identical for Ni or Fe interstitials and almost

identical for Ti interstitials. These configurations all involved split-interstitials with neighboring antisite defects. The antisite defects increase the migration energies of these alloys, because of the large number of atoms involved in the migration (the split-interstitials and the antisite defects). The associated antisite defects with the interstitial configurations also make migration using molecular statics difficult. The dumbbell arrangement as well as the associated antisite defects must be migrated together or in some reasonable order to achieve migration of the defect as a unit. Since the method of this migration was not obvious, migration of the interstitial defect was not done for either NiTi or FeTi.

An estimate of the interstitial formation energy can be made from the Frenkel pair formation energies and vacancy formation energies for each alloy. The Frenkel (a vacancy and interstitial defect combination) pair formation energies for FeTi are 4.34 eV for the Fe pair and 4.39 eV for the Ti pair (Table 7). The closeness of these values helps explain the similarity of the vacancy and interstitial configurations. Subtracting the vacancy formation energy from the Frenkel pair gives an estimate of the interstitial formation energy. The vacancy formation energy from Table 7 for FeTi is 1.07 eV and the interstitial formation energy is estimated to be between 3.2 eV and 3.3 eV. For NiTi

the Frenkel pair energies are 3.96 eV for the Ni pair and 4.42 eV for the Ti pair. The vacancy formation energy is 1.48 eV and the estimated interstitial formation energy is between 2.5 eV and 2.9 eV. This implies that interstitial defect formation in the FeTi lattice is more difficult (higher energy) than in the NiTi lattice with a difference in energy formation of 0.3 to 0.8 eV.

The interstitial configurations with a $\langle 111 \rangle$ oriented Ni-Ni or Fe-Fe dumbbell for NiTi and FeTi are similar to those found for CuTi and CuTi₂ (Shoemaker, et al., 1990, in press). Both the CuTi and CuTi₂ alloys have a Cu-Cu dumbbell (split-interstitials) centered on a Ti lattice site in the $\langle 111 \rangle$ unit vector direction with associated neighboring antisite defects. The exception to this configuration is the Fe interstitial configuration, because it is oriented in the $\langle 011 \rangle$ direction verses $\langle 111 \rangle$ for the other interstitials.

VIII. Conclusion

Atomistic simulation with a modified version of the DYNAMO code was used to calculate the point defect properties of the intermetallic compounds NiTi and FeTi. The calculated energies are believed to be experimentally accurate to within ± 0.1 eV.

The antisite pair formation energies for both alloys were calculated to be 1.015 eV for NiTi and 0.726 eV for FeTi. These values are more than twice the calculated formation energies of CuTi (0.385 eV) and CuTi₂ (0.460 eV). The high formation energies in NiTi explains why large amounts of energy are required for chemical disordering in the compound. The antisite defect and vacant Ni or Fe lattice sites were found to be weakly bound with a binding energy of 0.094 eV for NiTi and 0.055 eV for FeTi.

The stable vacancy defect configurations in both NiTi and FeTi were identical. Vacant Ni or Fe lattice sites were stable and preferred in the alloys with energy values of 6.356 eV for NiTi and 5.899 eV for FeTi. Ni and Fe vacancy migrations follow a six-jump ring sequence with energy barrier values calculated as 1.272 eV for NiTi and 1.737 eV for FeTi. Vacant Ti sites resulted in neighboring

antisite defects from migrating Ni or Fe atoms with energy values of 7.024 eV for NiTi and 6.336 eV for FeTi. The migrating Ni or Fe atoms to the Ti vacancies had migration barriers values of 0.134 eV for NiTi and 0.341 eV for FeTi. The vacancy defect formation energies were calculated from vacancy concentration values to be 1.48 eV for NiTi and 1.07 eV for FeTi.

The most stable interstitial defect configurations consisted of Ni-Ni or Fe-Fe split-interstitial dumbbells centered on a Ti site with one or two adjacent Ti antisite defects. The only difference between the two alloys was in the direction of the Ti interstitial dumbbell, whose Fe-Fe orientation was in the $\langle 011 \rangle$ direction. Ti interstitials resulted in two adjacent Ti antisite defects with a $\langle 011 \rangle$ direction Fe-Fe dumbbell or a $\langle 111 \rangle$ direction Ni-Ni dumbbell. The Ti interstitial formation energies were -2.395 eV for NiTi and -1.558 eV for FeTi. Ni or Fe interstitials both resulted in a single adjacent Ti antisite defect with Ni-Ni or Fe-Fe dumbbells oriented in the $\langle 111 \rangle$ direction. The Ni or Fe interstitial energies were -2.602 eV for NiTi and -1.945 eV for FeTi. Frenkel pair energies for NiTi were 3.961 and 4.422 eV for the Ni and Ti pair respectively. For FeTi the Frenkel pair formation energies were 4.341 and 4.391 eV for Fe and Ti pairs respectively.

APPENDIX A: Code Description and Sample Files

The following is a sample copy of an input file used in a molecular statics minimization calculation. A description of the RUNDYN code is also included for understanding of the code's basics (Sabochick, 1990, unpublished). Since the code is constantly being added to, this information is only a description of the RUNDYN version used for this work at this time.

THE CODE

The source file contains a computer code for doing molecular dynamics and molecular statics calculations using embedded-atom type potentials. The code is a modified version of the DYNAMO code, distributed by the Sandia group, with the following modifications:

- 1) The potential files (containing tables of the values for the components of the EAM potentials) have a different format.
- 2) The potentials are fitted within the code with cubic splines instead of Lagrange polynomials.
- 3) The code can do molecular statics calculations using a modified Fletcher-Powell minimization technique, which is faster than conjugate-gradients on large problems.

- 4) The code can now calculate migration energy barriers in a straight-forward manor.
- 5) Other special options have been added such as; atom switching, Frenkel pair generation, and Monte Carlo anti-site defect switching.

MIGRATION ENERGY TECHNIQUE

Migration energies are calculated by minimizing the system energy using the Fletcher-Powell method with a jumping atom constrained at various points along the migration path (Shoemaker, et al., 1990, in press). A reaction coordinate η is defined so that the points $r(\eta)$ along the migration path from r_1 to r_2 are specified by

$$r(\eta) = r_1 + \eta[r_2 - r_1] \quad (13)$$

The lattice system is then minimized with the jumping atom confined to a plane perpendicular to $r_2 - r_1$ at the point $r(\eta)$. The migration barrier energy $E(\eta)$ is then determined by repeating the calculation for various values of η , and the migration energy E_m is the maximum of $E(\eta)$ or η in the range -1 to 1 (i.e. -1.0, -0.75, -0.5, -0.25, 0.0, 0.25, 0.5, 0.75, and 1.0).

RUNNING THE CODE

The source code needs to be compiled and linked to a input file (in this case named `feti.inp`). A softlink was made to the RUNDYN source code in M. J. Sabochick's file directory. The input files could then be run by typing RUNDYN and the filename of the input file (i.e. `feti.inp`). The output file name (which is specified in the input file) is `feti.prn` for this example.

INPUT FILE DESCRIPTION

The following is a breakdown of the input file "`feti.inp`". The lines starting with `*****` and in bold print are the input file lines and the others are comments. At the beginning of each section is a header card of the form `$xyz` which helps the user delimit the sections. In the newest code version "RUNDYN2" the header cards and their contents can be omitted when the section is not used. In the previous version these header cards were checked by the code (routine `chkname()`) to make sure it was in the right place. Many of the data values in the input file are followed by a description (usually the name of the variable, which is set). These names are there just to help the user and are optional. All input lines start in column 1.

PRINT CONTROL OPTION:

```
***** $prntcard
Obsure options (not used in the calculations)
***** 0 ipinter
***** 0 ipatoms
***** -1 ipitera
Name of output file.
***** feti.prn
Name of restart save file (can be used to start another
run).
***** feti.res
Name of the trajectory save file.
***** none
Name of the energy information save file.
***** none
```

HEADER INFORMATION:

```
***** $headcard
Specific Run name for this calculation.
***** Setup of FeTi lattice
```

ENERGY POTENTIAL FOR RUN:

The potentials are referred to by numbers within the code; these numbers correspond to atom types. (i.e. 1 for Ni or Fe and 2 for Ti)

```
***** $funccard
Number of different potentials to be read in.
***** 2 ntypes
File Location &/Name(s) of the potential files (one on each
line.)
***** /enfacc1/enp/msabochi/Johnson/Pot/fe03.pot
***** /enfacc1/enp/msabochi/Johnson/Pot/ti20.pot
***** /enfacc1/enp/msabochi/Johnson/Pot/feti_05.pot
```

INITIALIZATION INFORMATION:

The code can start from a restart file written by a previous run, or generate a new lattice.

```
***** $initcard
Logical---whether or not to generate a lattice.
***** .true. genlat
Logical---whether or not to initialize velocities.
***** .true. genvel
Logical---whether or not to sort atoms according to distance from the origin.
***** .false. sort
Logical---name of start file where atom positions/velocities are.
***** none
```

LATTICE GENERATION INFORMATION: (only used if genlat equals true).

```
***** $latcard
Size of system in unit cells (x,y,z).
*****      8 8 8                      ncells
Unit cell dimensions. Diagonal matrix is a cubic or rectangular cell.
*****      2.976 0.000 0.000          basis (fitted a,
a=2.976)
*****      0.000 2.976 0.000
*****      0.000 0.000 2.976
Lower system boundaries. (x,y,z).
*****      0.0 0.0 0.0                perl b
Upper system boundaries. If values are < 0, they are automatically calculated from the information above.
*****      -1.0 -1.0 -1.0            perub
Number of atoms in a unit cell.
*****      2                          nc
Type & positions of atoms in unit cell, in unit cell coordinates(x,y,z).
*****      1 0.0 0.0 0.0              Ni or Fe type 1
*****      2 0.5 0.5 0.5              Ti          type 2
```

VELOCITY INITIALIZATION INFORMATION: (only used if genvel equal true).

```
***** $velcard
Temperature (Kelvin) to which the velocities are initialized.
*****      160.                      temp
```

SYSTEM BOUNDARY INFORMATION:

```
***** $bndcard
Boundary type. (1=fixed boundaries, 2=flexible, rectangular boundaries).
*****      2                          ibdtype
The following six variables are only used when ibdtype equal 2:
External applied pressure (in bars).
*****      0.0                      dpress
The following five variables are only used in dynamic calculations ($intcard): Boundary mass.
*****      1. 1. 1.                  bndmas
Drag (Automatically set if negative).
*****      -1. -1. -1.                bnddrg
Temperature setting option.
*****      1                          ifxtmp
Desired Temperature (Kelvin).
*****      160.                      destmp
Relaxation Time.
*****      0.100                     tmptim
```


Option to use Images.

***** .false.

whether or not to use

images

NEIGHBOR OPTIONS:

***** \$neicard

Neighbor list used? (1=no, 2=yes).

***** 2

nmeth

Cutoff radius (Angstroms) for neighbor list (only used if nmeth equal=2).

***** 1.0

dradn

DEFECT INFORMATION: (move atoms, create interstitials/vacancies).

***** \$defcard

Defect type. (-1=vacancy, 0=end of list, 1=interstitial, 99=not used).

***** 99

ktype

Atom position (x,y,z).

***** 0.0 0.0 0.0

pos

Atom velocity (x,y,z).

***** 0.0 0.0 0.0

vel

Atom number to delete for vacancy.

***** 0

num

TRAJECTORY INFORMATION:

***** \$trajsave

***** -1

save interval

Option to save position or position & velocity.

***** 1

what is saved (1=pos

only, 2=pos and vel)

FORCED "STATIC MIGRATION" MODIFICATIONS: (added to determine migration energy).

***** \$modcard

Option (0=Off, 1=On)

***** 0

Number of Neighboring Gate atoms.

***** 6

First # is Migration atom the remaining are a list of gate atom numbers.

***** 440 568 456 442 457 569 583

Percent Distance η (+or-) from Midpoint $r(\eta)$ (0.0), Distance(A^0), Constant.

***** -0.25 1.2582 1.0e+4

Unit Vector Direction (x'-x,y'-y,z'-z) from Position (x,y,z) to (x',y',z').

***** 1.0 1.0 1.0

MONTE CARLO ATOM SWITCHING INFORMATION: (used in dynamic calculations)

```
**** $swicard
***** -1 kbswit
***** -2
Antisite Defect Energy (eV) Fe Atom on Ti Site.
***** 0.4910
Antisite Defect Energy (eV) Ti Atom on Fe Site.
***** 0.2352
```

FRENKEL PAIR CREATION INFORMATION:

```
***** $frencard
Option (-1=Off)
***** -1
***** 0.7
***** 1
***** 1
***** 5.0
***** 10.0
```

SPECIFICATION OF RUN TYPE: (dynamic, static)

```
***** $intcard
Type of Integrator/Minimizer.
      ( 1 = Dynamic Gear predictor-corrector)
      (-1 = Static Conjugate-gradients Minimizer)
      (-2 = Static Fletcher-Powell Minimizer)
      (1000 = Dynamic Monte Carlo Switching & Pred/Corr)
***** -2 inte
Equilibrium Steps (Dynamic runs).
***** 300 equilibrium steps
Property Steps (Dynamic runs).
***** 5000 property steps
Output Interval (Dynamic runs).
***** 10 print interval
Accuracy Option (Dynamic runs).
***** 0 iaccur
Time Step (Dynamic runs).
***** 0.001 dt
Convergence tolerance (Static Minimization runs).
***** 1.e-13 tol
Maximum number of force evaluations.
***** 100000 nfmax
```

APPENDIX B: Calculation Spreadsheet Results

The following tables are a copy of a Lotus 123 spreadsheet file (MIGRATE.WK1) used to record and manipulate the calculated lattice configuration energies. This data was used to create the various graphs and tables given in the text. The system energies are given untruncated for completeness and although seven digits are given, only 3 are considered significant (Sabochnik, 1990, personal conversion). In repeat calculations seven significant digits could be duplicated, if the tolerance was input as $1.0E-13$ (see Appendix A).

Table 8. FeTi "Ti" Vacancy MIGRATION (Min = -5002.1175360)

%Distance	Energy (eV)	Difference
0.0000000	-5001.0895532	1.0279828
0.1250000	-5000.9724442	1.1450918
0.2500000	-5000.7488333	1.3687027
0.3750000	-5000.7767544	1.3407816
0.5000000	-5001.0400101	1.0775259
0.6250000	-5001.2847346	0.8328014
0.7500000	-5001.6757710	0.4417650
0.8750000	-5002.0145435	0.1029925
1.0000000	-5002.1175360	0.0000000

Table 9. NiTi "Ti" Vacancy MIGRATION (Min = -5113.8368959)

%Distance	Energy (eV)	Difference
0.0000000	-5113.6320329	0.2048630
0.1250000	-5113.6103820	0.2265139
0.2500000	-5113.5446613	0.2922346
0.3750000	-5113.5031555	0.3337404
0.5000000	-5113.4976717	0.3392242
0.6250000	-5113.5384801	0.2984158
0.7500000	-5113.6303356	0.2065603
0.8750000	-5113.7620650	0.0748309
1.0000000	-5113.8368959	0.0000000

Table 10. FeTi "Fe" Vacancy MIGRATION (Min=-5002.5538190)

%Distance	Direct Data1 (eV)	Difference1	InDirect Data2 (eV)	Difference2
0.000000	-5002.5538190	0.000000	-5002.5538190	0.000000
0.125000			-5002.4249982	0.1288208
0.250000			-5002.0935009	0.4603181
0.375000			-5001.7810563	0.7727627
0.500000			-5001.5660417	0.9877773
0.625000			-5001.4077289	1.1460901
0.750000	-5001.9887234	0.5650956	-5001.3482255	1.2055935
0.875000			-5001.3337781	1.2200409
1.000000			-5001.1862555	1.3675635
1.125000			-5001.1988910	1.3549280
1.250000			-5000.9026331	1.6511859
1.375000			-5000.8156227	1.7381963
1.500000	-5001.2153024	1.3385166	-5000.9899902	1.5638288
1.625000			-5001.1942688	1.3595502
1.750000			-5001.5566586	0.9971604
1.875000			-5001.8630311	0.6907879
2.000000			-5001.9657553	0.5880637
2.125000			-5001.8229103	0.7309087
2.250000	-5000.4420590	2.1117600	-5001.5385912	1.0152278
2.375000			-5001.3129838	1.2408352
2.500000			-5001.2175267	1.3362923
2.625000			-5001.2152742	1.3385448
2.750000			-5001.3265066	1.2273124
2.875000			-5001.4552516	1.0985674
3.000000	-5000.1981781	2.3556409	-5001.4637261	1.0900929
3.125000			-5001.4271793	1.1266397
3.250000			-5001.2948665	1.2589525
3.375000			-5001.2102149	1.3436041
3.500000			-5001.2176036	1.3362154
3.625000			-5001.2994210	1.2543980
3.750000	-5000.4379935	2.1158255	-5001.4815633	1.0722557
3.875000			-5001.7413968	0.8124222
4.000000			-5001.9657552	0.5880638
4.125000			-5001.8555345	0.6982845
4.250000			-5001.5487642	1.0050548
4.375000			-5001.1911098	1.3627092
4.500000	-5001.2084583	1.3453607	-5000.9899979	1.5638211
4.625000			-5000.8166164	1.7372026
4.750000			-5000.8983959	1.6554231

4.8750000			-5001.1894443	1.3643747
5.0000000			-5001.1864245	1.3673945
5.1250000			-5001.3338043	1.2200147
5.2500000	-5001.9840768	0.5697422	-5001.3482314	1.2055876
5.3750000			-5001.4077468	1.1460722
5.5000000			-5001.5660416	0.9877774
5.6250000			-5001.7810170	0.7728020
5.7500000			-5002.0931025	0.4607165
5.8750000			-5002.4248725	0.1289465
6.0000000	-5002.5538138	0.0000052	-5002.5538185	0.0000005

Table 11. NiTi "Ni" Vacancy MIGRATION (Min=-5114.5049341)

%Distance	Direct Data1 (eV)	Difference1	InDirect Data2 (eV)	Difference2
0.000000	-5114.5049341	0.0000000	-5114.5049341	0.0000000
0.125000			-5114.3898139	0.1151202
0.250000			-5114.1423992	0.3625349
0.375000			-5113.9338859	0.5710482
0.500000			-5113.8152596	0.6896745
0.625000			-5113.7637272	0.7412069
0.750000	-5114.1389165	0.3660176	-5113.7643917	0.7405424
0.875000			-5113.7823340	0.7226001
1.000000			-5113.7839404	0.7209937
1.125000			-5113.7337982	0.7711359
1.250000			-5113.6136335	0.8913006
1.375000			-5113.5094827	0.9954514
1.500000	-5113.5338844	0.9710497	-5113.4481337	1.0568004
1.625000			-5113.4476692	1.0572649
1.750000			-5113.5085847	0.9963494
1.875000			-5113.6265550	0.8783791
2.000000			-5113.7095138	0.7954203
2.125000			-5113.5930761	0.9118580
2.250000	-5113.0467984	1.4581357	-5113.3886236	1.1163105
2.375000			-5113.2578421	1.2470920
0.000000			-5113.2331188	1.2718153
2.625000			-5113.3017706	1.2031635
2.750000			-5113.4426337	1.0623004
2.875000			-5113.5775667	0.9273674
3.000000	-5112.8455693	1.6593648	-5113.5894853	0.9154488
3.125000			-5113.5508028	0.9541313
3.250000			-5113.4123014	1.0926327
3.375000			-5113.2914537	1.2134804
3.500000			-5113.2331181	1.2718160
3.625000			-5113.2515763	1.2533578
3.750000	-5113.0467884	1.4581457	-5113.3547116	1.1502225
3.875000			-5113.5363502	0.9685839
4.000000			-5113.7095137	0.7954204
4.125000			-5113.6438446	0.8610895
4.250000			-5113.5184936	0.9864405
4.375000			-5113.4489913	1.0559428
4.500000	-5113.5338719	0.9710622	-5113.4481258	1.0568083
4.625000			-5113.5134446	0.9914895
4.750000			-5113.6249491	0.8799850

4.8750000			-5113.7477682	0.7571659
5.0000000			-5113.7839404	0.7209937
5.1250000			-5113.7823341	0.7226000
5.2500000	-5114.1389188	0.3660153	-5113.7643917	0.7405424
5.3750000			-5113.7637272	0.7412069
5.5000000			-5113.8152596	0.6896745
5.6250000			-5113.9388490	0.5660851
5.7500000			-5114.1423971	0.3625370
5.8750000			-5114.3898138	0.1151203
6.0000000	-5114.5049341	0.0000000	-5114.5049341	0.0000000

Table 12. Stable Defect Configuration Energies Results
($E = U - U_0$)

Nickel Titanium (NiTi)

System	Energy(eV)	Difference(eV)
-----	-----	-----
(U)	(U)	(E)
Perfect Crystal (U_0)	-5120.8607297	0.0000000
Ni Antisite Defect	-5120.0983898	0.7623399
Ti Antisite Defect	-5120.6076298	0.2530999
NiTi Antisite Formation		0.5092400
NiTi Antisite Pair		1.0154398
Ni Vacancy Defect	-5114.5049341	6.3557956
Ti Vacancy Defect	-5113.8368959	7.0238338
NiTi Vacancy Formation		1.4800000
Ni Interstitial Defect	-5123.2559795	-2.3952498
Ti Interstitial Defect	-5123.4626653	-2.6019356
Ni Frenkel Pair in NiTi		3.9605458
Ti Frenkel Pair in NiTi		4.4218982

Iron Titanium (FeTi)

System	Energy(eV)	Difference(eV)
-----	-----	-----
(U)	(U)	(E)
Perfect Crystal (U_0)	-5008.4530840	0.0000000
Fe Antisite Defect	-5007.9620535	0.4910305
Ti Antisite Defect	-5008.2178813	0.2352027
FeTi Antisite Formation		0.2558278
FeTi Antisite Pair		0.7262332
Fe Vacancy Defect	-5002.5538190	5.8992650
Ti Vacancy Defect	-5002.1175360	6.3355480
FeTi Vacancy Formation		1.0700000
Fe Interstitial Defect	-5010.0113699	-1.5582859
Ti Interstitial Defect	-5010.3980165	-1.9449325
Fe Frenkel Pair in FeTi		4.3409791
Ti Frenkel Pair in FeTi		4.3906155

APPENDIX C: Vacancy Formation Energy Code

The following program was written using TK Solver Plus software version 1.1. Eight unknowns N^{Ni} , N^{Ti} , n_a^{Ni} , n_v^{Ni} , n_a^{Ti} , n_v^{Ti} , μ^{Ni} , and μ^{Ti} are solved by the eight equations (8a,8b), (9a,9b), (10a,10b), (11), (12), and their complements as presented in section V. A list of guessed values are input into the program for each of the unknowns for each temperature of interest. The only required input values to the program are the five total system energies for the global minimum configurations and the number of lattice sites for each type of atom in the compound. These energies include the perfect crystal U_0 for each alloy, the antisite defect total system energies for NiTi U_a^{Ni}, U_a^{Ti} or for FeTi U_a^{Fe}, U_a^{Ti} (Table 1), plus the vacancy defect total system energies for NiTi U_v^{Ni}, U_v^{Ti} or for FeTi U_v^{Fe}, U_v^{Ti} (Table 3).

The program is written using nomenclature of the NiTi lattice. This same approach was used in the presentation of the equations in section V. The program is however generic and can be used for any type of compound.

===== VARIABLE SHEET ===== For Academic Use Only
 St Input Name Output Unit Comment=====

 TK Solver Program Ver5.4 12Dec90

 Calculates the effective vacancy
 formation energy, using Foiles
 & Daw method(J.Mat.Res.2,3,1987)
 File: ENERGY.TK by Tom Lutton

INPUT TEMPERATURE:

L T 1200 K Temperature (Kelvin)
 L .83333 TInv 1/K Temperature Inverse = 1000/T

OUTPUT:

L Cv 3.0E-7 Concentration of Vacancy Defect

GUESS INPUT VALUES:

LG 2.9E-7 n_Ni_v Atom fraction Ni Vacancy Defect
 LG 5.5E-9 n_Ti_v Atom fraction Ti Vacancy Defect
 LG .00366 n_Ni_a Atom fraction Ni Antisite Defect
 LG .00366 n_Ti_a Atom fraction Ti Antisite Defect
 LG -4.874 muNi eV Chemical Potential of.....Ni
 LG -5.128 muTi eV Chemical Potential of.....Ti
 LG 511.99 N_Ni # Lattice Sites(@given T)Ni
 LG 511.99 N_Ti # Lattice Sites(@given T)Ti

INPUT:

Chart of Nuclides(k=8.61735E-5)
 8.6E-5 k eV/K Boltzmann Constant (eV/Kelvin)
 1024 Ns Total # Lattice Sites(@ T=0)
 512 nsNi # Lattice Sites(@ T=0) of Ni
 512 nsTi # Lattice Sites(@ T=0) of Ti
 fsNi .5 Fraction of Ni Lattice Sites
 fsTi .5 Fraction of Ti Lattice Sites
 i 2 Inverse Fraction = 1/fsNi
 j 2 Inverse Fraction = 1/fsTi

INPUT ENERGIES:

-5120.9 Uo eV NiTi System Energy Perfect Cryst
 -5120.1 U_Ni_a eV NiTi System Energy Ni Antisite
 -5120.6 U_Ti_a eV NiTi System Energy Ti Antisite
 -5114.5 U_Ni_v eV NiTi System Energy Ni Vacancy
 -5113.8 U_Ti_v eV NiTi System Energy Ti Vacancy

OUTPUTS:

E_Ni_a .7623 eV NiTi...Energy of Ni Antisite Def

E_Ti_a .2530 eV NiTi...Energy of Ti Antisite Def
 E_Ni_v 6.355 eV NiTi...Energy of Ni Vacancy Def
 E_Ti_v 7.023 eV NiTi...Energy of Ti Vacancy Def

U -5117. eV NiTi Total System Energy Ns Site
 S 44.32 eV/K Configuration Entropy NiTi Syste

Ideal entropy Function

s1 .0432 eV/K Term #1
 s2 9.1E-6 eV/K Term #2
 s3 .0433 eV/K Term #3
 s4 2.1E-7 eV/K Term #4

OUTPUT:

Vacancy
 L Efxslop Energy Formation= $-k \ln(Cv)/T^{-1}$
 NOTE: The following values
 are output initially&later
 used as inputs (see Rules).
 L TInv1 .8333 Dummy List Offset TInv by 1
 L Cv1 3.0E-7 Dummy List Offset Cv by 1

INPUT VALUES:

-5120.8607	NiTi System Energy..Perfect Crystal
-5120.0984	NiTi System Energy..Ni Antisite Defect
-5120.6076	NiTi System Energy..Ti Antisite Defect
-5114.5045	NiTi System Energy..Ni Vacancy Defect
-5113.8369	NiTi System Energy..Ti Vacancy Defect

Note: Ns=1024 nsNi=512 nsTi=512

-5008.4531	FeTi System Energy..Perfect Crystal
-5007.9621	FeTi System Energy..Ni Antisite Defect
-5008.2179	FeTi System Energy..Ti Antisite Defect
-5002.5538	FeTi System Energy..Ni Vacancy Defect
-5002.1175	FeTi System Energy..Ti Vacancy Defect

Note: Ns=1024 nsFe=512 nsTi=512

-4404.4207	CuTi System Energy..Perfect Crystal
-4403.0266	CuTi System Energy..Ni Antisite Defect
-4405.4299	CuTi System Energy..Ti Antisite Defect
-4399.6440	CuTi System Energy..Ni Vacancy Defect
-4398.4100	CuTi System Energy..Ti Vacancy Defect

Note: Ref Case used k=8.615E-5

Note: Ns=1024 nsCu=512 nsTi=512

-3965.5986	CuTi2 System Energy Perfect Crystal
-3964.3864	CuTi2 System Energy Ni Antisite Defect
-3966.3511	CuTi2 System Energy Ti Antisite Defect
-3960.8716	CuTi2 System Energy Ni Vacancy Defect
-3959.7368	CuTi2 System Energy Ti Vacancy Defect

Note: Ref Case used k=8.615E-5

Note: Ns=882 nsCu=294 nsTi=588

===== RULE SHEET ===== For Academic Use Only
S Rule=====

"Equations for NiTi Effective Vacancy Formation Energy

*****TOTAL VACANCY CONCENTRATION:*****

$$C_v = n_{Ni_v} + n_{Ti_v}$$

*****INVERSE TEMPERATURE:*****

$$T_{Inv} = 1000 / T$$

*****INPUT (Total System Energy)-(Perfect Crystal Energy)

$$E_{Ti_a} = U_{Ti_a} - U_o$$

$$E_{Ni_a} = U_{Ni_a} - U_o$$

$$E_{Ti_v} = U_{Ti_v} - U_o$$

$$E_{Ni_v} = U_{Ni_v} - U_o$$

*****INPUT of Number of Lattice Sites of Each Element:****

$$fs_{Ni} = ns_{Ni} / (ns_{Ni} + ns_{Ti})$$

$$fs_{Ti} = ns_{Ti} / (ns_{Ni} + ns_{Ti})$$

*****EQUATION..(1)*****

$$n_{Ni_v} = fs_{Ni} * (\exp(-(E_{Ni_v} + \mu_{Ni}) / (k * T))) / (1 + \exp(-(E_{Ni_v} + \mu_{Ni}) / (k * T)))$$

*****EQUATION..(2)*****

$$n_{Ti_v} = fs_{Ti} * (\exp(-(E_{Ti_v} + \mu_{Ti}) / (k * T))) / (1 + \exp(-(E_{Ti_v} + \mu_{Ti}) / (k * T)))$$

*****EQUATION..(3)*****

$$n_{Ni_a} = fs_{Ti} * (\exp(-(E_{Ni_a} + \mu_{Ti} - \mu_{Ni}) / (k * T))) / (1 + \exp(-(E_{Ni_a} + \mu_{Ti} - \mu_{Ni}) / (k * T)))$$

*****EQUATION..(4)*****

$$n_{Ti_a} = fs_{Ni} * (\exp(-(E_{Ti_a} + \mu_{Ni} - \mu_{Ti}) / (k * T))) / (1 + \exp(-(E_{Ti_a} + \mu_{Ni} - \mu_{Ti}) / (k * T)))$$

*****EQUATION..(5)*****

$$N_{Ni} = N_s * (fs_{Ni} - n_{Ni_v} + n_{Ni_a} - n_{Ti_a})$$

*****EQUATION..(6)*****

```
N_Ti = Ns * (fsTi - n_Ti_v + n_Ti_a - n_Ni_a)
```

```
"*****EQUATION..(7)*****"
```

```
fsNi = N_Ni / (N_Ni + N_Ti)
```

```
"*****EQUATION..(8)*****"
```

```
U - (k*T*S) = (muNi*N_Ni) + (muTi*N_Ti)
```

```
"WHERE:
```

```
U =Uo+Ns*(n_Ni_v*E_Ni_v + n_Ti_v*E_Ti_v + n_Ni_a*E_Ni_a +
                                         n_Ti_a*E_Ti_a)
```

```
S =Ns * ((fsNi)*(s1+s2) + (fsTi)*(s3+s4))
```

```
            i=1/fsNi  "Temporary Term
```

```
            j=1/fsTi  "Temporary Term
```

```
    If n_Ti_a>0  then s1= -((i*n_Ti_a)*ln(i*n_Ti_a)+
                           (1-i*n_Ti_a) * ln(1-i*n_Ti_a))
```

```
*If n_Ti_a<=0 then s1= 0
```

```
    If n_Ni_v>0  then s2= -((i*n_Ni_v)*ln(i*n_Ni_v)+
                           (1-i*n_Ni_v) * ln(1-i*n_Ni_v))
```

```
*If n_Ni_v<=0 then s2= 0
```

```
    If n_Ni_a>0  then s3= -((j*n_Ni_a)*ln(j*n_Ni_a)+
                           (1-j*n_Ni_a) * ln(1-j*n_Ni_a))
```

```
*If n_Ni_a<=0 then s3= 0
```

```
    If n_Ti_v>0  then s4= -((j*n_Ti_v)*ln(j*n_Ti_v)+
                           (1-j*n_Ti_v)*ln(1-j*n_Ti_v))
```

```
*If n_Ti_v<=0 then s4= 0
```

"Note: The If statements were added to help cure natural log errors, which occur when the atom fraction values go negative during iteration. The negative values occur when errors become larger than the tolerances of the iterations. Final values must be positive. This is not a solution to the problem of log errors, but a symptom of low tolerances. Solutions include changing the input guess values, changing the tolerance (default=1E-6), and changing the form of the equations. In general, changing the equation doesn't effect results. The first solution is not always correct; change tolerances and test the solution. Problems with "too many guesses", negative atom fraction values, inconsistency, and more than one solution are all symptoms of low tolerances compared to errors. For understanding the problems read the TK Solver help sections on the iterative solver.

The problems are mostly with the antisite defect atom fractions and they become more pronounced with lower temperatures. Thus, to solve these equations it is best to start with a higher temperature input (1200 Kelvin) and find a solution. Use the guess values given in the variable sheet to start with. Then use the results as input to the next lower temperature of interest. This ensures reasonable input values. As solution errors appear lower the tolerance. At some point the errors are so small compared to the tolerances, that no solution is possible with TK. At these low temperatures, the values are generally not realistic and the process can be stopped.

```
*****
"*For List Solutions VACANCY FORMATION ENERGY(Ef)= -k*slope
*****
>Note: First calculate Cv & TInv valves. Then offset these
values by 1 space value at top of each list. Next cancel
the TInv= & Cv= rules & uncanceled the Efxslope rule to do
the calculation. Be sure to change Cv, Cv1, TInv1, & TInv
to list Inputs.
```

```
C TInv = TInv1
Cv      = Cv1
C Efxslope= -k * (ln(Cv1)-ln(Cv)) / ((TInv1-TInv)/1000)
```

```
===== UNIT SHEET ===== For Academic Use Only
From===== To===== Multiply By====Add Offset====Comment=====
K           C                    -273.15
C           F                    32
K           F                    1.8
K           F                    1.8
eV/K        eV*K^-1
eV/K*K      eV
```

```
===== GLOBAL SHEET ===== For Academic Use Only
Display Intermediate Values: Yes
Stop on List Error:          No
Use Automatic Iteration:     Yes
Comparison Tolerance:       1E-10
Typical Value:               1
Maximum Iteration Count:     25
```


Table 13. Vacancy Concentration of NiTi

T(K)	K ⁻¹	n _{Ni_v}	n _{Ti_v}	n _{Ni_a}	n _{Ti_a}	muNi	muTi	NNi
10000	.1	.12827163	.09360703	.18717	.16984	-5.43	-5.75	398
5000	.2	.02036074	.00826969	.12072	.11468	-4.99	-5.26	497
3333	.3	.00333461	.00080280	.07356	.07229	-4.91	-5.17	510
2500	.4	.00056144	8.2722E-5	.04339	.04315	-4.89	-5.14	512
2000	.5	9.6792E-5	8.8014E-6	.02499	.02494	-4.88	-5.13	512
1667	.6	1.6952E-5	9.5332E-7	.01417	.01416	-4.87	-5.13	512
1429	.7	2.9973E-6	1.0430E-7	.00796	.00796	-4.87	-5.13	512
1250	.8	5.3287E-7	1.1477E-8	.00445	.00445	-4.87	-5.12	512
1200	.83	2.9987E-7	5.5038E-9	.00366	.00366	-4.87	-5.12	512
1111	.9	9.5034E-8	1.2668E-9	.00248	.00248	-4.87	-5.12	512
1000	1	1.6978E-8	1.401E-10	.00138	.00138	-4.87	-5.12	512
909.1	1.1	3.0362E-9	1.550E-11	.00076	.00076	-4.87	-5.12	512
833.3	1.2	5.433E-10	1.717E-12	.00042	.00042	-4.87	-5.12	512
750	1.3	5.480E-11	9.136E-14	.00019	.00019	-4.87	-5.12	512
714.3	1.4	1.741E-11	2.107E-14	.00013	.00013	-4.87	-5.12	512
666.7	1.5	3.116E-12	2.335E-15	7.3E-5	7.3E-5	-4.87	-5.12	512
571.4	1.7	4.227E-14	9.546E-18	1.7E-5	1.7E-5	-4.87	-5.12	512
545.5	1.8	1.008E-14	1.526E-18	.00001	.00001	-4.87	-5.12	512
500	2	5.734E-16	4.033E-20	3.8E-6	3.8E-6	-4.87	-5.12	512
444.4	2.2	7.765E-18	1.078E-20	8.7E-7	8.7E-7	-4.87	-5.12	512
428.6	2.3	1.751E-18	2.981E-20	5.4E-7	5.4E-7	-4.87	-5.12	512
400	2.5	6.838E-20	3.542E-20	2.0E-7	2.0E-7	-4.87	-5.12	512
363.6	2.7	1.166E-21	2.838E-22	4.6E-8	4.6E-8	-4.87	-5.12	512
352.9	2.8	2.612E-21	-2.27E-21	2.8E-8	2.8E-8	-4.87	-5.12	512
333.3	3	-1.81E-19	2.205E-20	1.1E-8	1.1E-8	-4.87	-5.12	512
307.7	3.2	-3.55E-17	-2.95E-19	2.4E-9	2.4E-9	-4.87	-5.12	512
300	3.3	-6.21E-17	-2.18E-20	1.5E-9	1.5E-9	-4.87	-5.12	512
285.7	3.5	3.371E-16	7.154E-19	6E-10	6E-10	-4.87	-5.12	512

Key:

T = Temperature in Kelvin

K⁻¹ = Inverse Temperature * 1000 in 1/Kelvin

CvNiTi = Total Vacancy Concentration

n_{Ni_v} or n_{Ti_v} = Ni or Ti Vacancy Concentration Fractionn_{Ni_a} or n_{Ti_a} = Ni or Ti Antisite Defect Concentration Fraction

muNi or muTi = Ni or Ti Chemical Potential

NNi = Ni or Ti Number of lattice sites at a given Temperature (T)

Table 14. Vacancy Concentration of FeTi

T(K)	K ⁻¹	n_Fe_v	n_Ti_v	n_Fe_a	n_Ti_a	muFe	muTi	NFe
10000	.1	.21754061	.18324654	.20673	.18958	-5.67	-5.86	307
5000	.2	.05608482	.03077715	.15688	.14423	-5.00	-5.16	468
3333	.3	.01498607	.00537199	.11255	.10775	-4.90	-5.03	502
2500	.4	.00405130	.00098554	.07895	.07742	-4.86	-4.99	509
2000	.5	.00111089	.00018685	.05445	.05398	-4.84	-4.97	511
1667	.6	.00030883	.00003617	.03702	.03688	-4.83	-4.96	512
1429	.7	8.6802E-5	7.0972E-6	.02490	.02486	-4.83	-4.96	512
1250	.8	2.4594E-5	1.4051E-6	.01661	.01660	-4.83	-4.95	512
1200	.83	1.6175E-5	8.2012E-7	.01450	.01449	-4.83	-4.95	512
1111	.9	7.0072E-6	2.7985E-7	.01102	.01102	-4.82	-4.95	512
1000	1	2.0041E-6	5.5955E-8	.00729	.00729	-4.82	-4.95	512
909.1	1.1	5.7465E-7	1.1218E-8	.00481	.00481	-4.82	-4.95	512
833.3	1.2	1.6506E-7	2.2527E-9	.00316	.00316	-4.82	-4.95	512
750	1.3	3.1333E-8	2.654E-10	.00181	.00181	-4.82	-4.95	512
714.3	1.4	1.3658E-8	9.112E-11	.00137	.00137	-4.82	-4.95	512
666.7	1.5	3.9322E-9	1.834E-11	.00090	.00090	-4.82	-4.95	512
571.4	1.7	1.751E-10	3.339E-13	.00031	.00031	-4.82	-4.95	512
545.5	1.8	6.207E-11	8.784E-14	.00022	.00022	-4.82	-4.95	512
500	2	7.803E-12	6.082E-15	.00011	.00011	-4.82	-4.95	512
444.4	2.2	3.478E-13	1.108E-16	3.8E-5	3.8E-5	-4.82	-4.95	512
428.6	2.3	1.233E-13	2.916E-17	2.7E-5	2.7E-5	-4.82	-4.95	512
400	2.5	1.550E-14	2.019E-18	1.3E-5	1.3E-5	-4.82	-4.95	512
363.6	2.7	6.912E-16	3.681E-20	4.6E-6	4.6E-6	-4.82	-4.95	512
352.9	2.8	2.451E-16	9.662E-21	3.3E-6	3.3E-6	-4.82	-4.95	512
333.3	3	3.081E-17	4.874E-22	1.6E-6	1.6E-6	-4.82	-4.95	512
307.7	3.2	1.411E-18	3.762E-20	5.6E-7	5.6E-7	-4.82	-4.95	512
300	3.3	4.578E-19	1.788E-21	4.0E-7	4.0E-7	-4.82	-4.95	512
285.7	3.5	1.626E-19	9.35E-20	2.0E-7	2.0E-7	-4.82	-4.95	512

Key:

T = Temperature in Kelvin

K⁻¹ = Inverse Temperature * 1000 in 1/Kelvin

CvFeTi = Total Vacancy Concentration

n_Fe_v or n_Ti_v = Fe or Ti Vacancy Concentration Fraction

n_Fe_a or n_Ti_a = Fe or Ti Antisite Defect Concentration Fraction

muFe or muTi = Fe or Ti Chemical Potential

NFe = Fe or Ti Number of lattice sites at a given Temperature (T)

Table 15. Vacancy Concentration of CuTi

T(K)	K ⁻¹	n_Cu_v	n_Ti_v	n_Cu_a	n_Ti_a	muCu	muTi	NCu
10000	.1	.25516498	.25142088	.22314	.22126	-4.81	-6.02	253
5000	.2	.06687083	.06307794	.19603	.19413	-3.97	-5.17	445
3333	.3	.01776014	.01598982	.16969	.16881	-3.82	-5.03	495
2500	.4	.00475944	.00410771	.14538	.14505	-3.77	-4.97	507
2000	.5	.00128679	.00106767	.12337	.12326	-3.75	-4.95	511
1667	.6	.00035093	.00028025	.10378	.10374	-3.73	-4.93	512
1429	.7	9.6472E-5	7.4187E-5	.08659	.08658	-3.72	-4.92	512
1250	.8	2.6709E-5	1.9781E-5	.07175	.07174	-3.71	-4.91	512
1200	.83	1.7432E-5	.00001275	.06729	.06729	-3.71	-4.91	512
1111	.9	7.4397E-6	5.3068E-6	.05908	.05908	-3.71	-4.91	512
1000	1	2.0831E-6	1.4311E-6	.04840	.04840	-3.70	-4.91	512
909.1	1.1	5.8583E-7	3.8765E-7	.03948	.03948	-3.70	-4.90	512
833.3	1.2	1.6535E-7	1.0538E-7	.03208	.03208	-3.70	-4.90	512
750	1.3	3.0755E-8	1.8644E-8	.02422	.02422	-3.70	-4.90	512
714.3	1.4	1.3285E-8	7.8543E-9	.02101	.02101	-3.70	-4.90	512
666.7	1.5	3.7778E-9	2.1512E-9	.01695	.01695	-3.70	-4.90	512
571.4	1.7	1.640E-10	8.501E-11	.00984	.00984	-3.70	-4.90	512
545.5	1.8	5.772E-11	2.900E-11	.00820	.00820	-3.70	-4.90	512
500	2	7.161E-12	3.380E-12	.00568	.00568	-3.70	-4.90	512
444.4	2.2	3.139E-13	1.349E-13	.00326	.00326	-3.70	-4.90	512
428.6	2.3	1.107E-13	4.611E-14	.00271	.00271	-3.70	-4.90	512
400	2.5	1.379E-14	5.393E-15	.00187	.00187	-3.70	-4.90	512
363.6	2.7	6.062E-16	2.159E-16	.00107	.00107	-3.70	-4.90	512
352.9	2.8	2.140E-16	7.387E-17	.00089	.00089	-3.70	-4.90	512
333.3	3	2.667E-17	8.646E-18	.00061	.00061	-3.70	-4.90	512
307.7	3.2	1.174E-18	3.466E-19	.00035	.00035	-3.70	-4.90	512
300	3.3	4.146E-19	1.186E-19	.00029	.00029	-3.70	-4.90	512
285.7	3.5	5.125E-20	1.353E-20	.00020	.00020	-3.70	-4.90	512

Key:

T = Temperature in Kelvin

K⁻¹ = Inverse Temperature * 1000 in 1/Kelvin

CvCuTi = Total Vacancy Concentration

n_Cu_v or n_Ti_v = Cu or Ti Vacancy Concentration Fraction

n_Cu_a or n_Ti_a = Cu or Ti Antisite Defect Concentration Fraction

muCu or muTi = Cu or Ti Chemical Potential

NCu = Cu or Ti Number of lattice sites at a given Temperature (T)

Table 16. Vacancy Concentration CuTi₂

T(K)	K ⁻¹	n_Cu_v	n_Ti_v	n_Cu_a	n_Ti_a	muCu	muTi2	NCu
10000	.1	.21562640	.32798014	.21719	.18277	-5.24	-5.83	134
5000	.2	.07974555	.08346786	.18367	.15833	-4.22	-5.02	246
3333	.3	.02803006	.02225664	.14880	.13753	-4.04	-4.89	279
2500	.4	.00954481	.00616024	.12062	.11631	-3.96	-4.85	289
2000	.5	.00322218	.00174452	.09762	.09605	-3.92	-4.83	293
1667	.6	.00109218	.00050101	.07850	.07794	-3.90	-4.82	294
1429	.7	.00037326	.00014527	.06263	.06243	-3.89	-4.82	294
1250	.8	.00012866	4.2427E-5	.04958	.04951	-3.88	-4.82	294
1200	.83	9.0371E-5	2.8185E-5	.04579	.04574	-3.87	-4.82	294
1111	.9	4.4689E-5	.00001246	.03899	.03896	-3.87	-4.81	294
1000	1	1.5621E-5	3.6756E-6	.03048	.03048	-3.86	-4.81	294
909.1	1.1	5.4880E-6	1.0881E-6	.02373	.02373	-3.86	-4.81	294
833.3	1.2	1.9360E-6	3.2300E-7	.01840	.01840	-3.86	-4.81	294
750	1.3	4.8489E-7	6.4175E-8	.01306	.01306	-3.85	-4.81	294
714.3	1.4	2.4306E-7	2.8637E-8	.01098	.01098	-3.85	-4.81	294
666.7	1.5	8.6398E-8	8.5456E-9	.00846	.00846	-3.85	-4.81	294
571.4	1.7	6.5463E-9	4.174E-10	.00438	.00438	-3.85	-4.81	294
545.5	1.8	2.7736E-9	1.527E-10	.00352	.00352	-3.85	-4.81	294
500	2	4.985E-10	2.046E-11	.00226	.00226	-3.85	-4.81	294
444.4	2.2	3.806E-11	1.004E-12	.00116	.00116	-3.85	-4.81	294
428.6	2.3	1.615E-11	3.679E-13	.00093	.00093	-3.85	-4.81	294
400	2.5	2.910E-12	4.936E-14	.00060	.00060	-3.84	-4.82	294
363.6	2.7	2.226E-13	2.427E-15	.00031	.00031	-3.84	-4.82	294
352.9	2.8	9.451E-14	8.892E-16	.00025	.00025	-3.84	-4.82	294
333.3	3	1.704E-14	1.194E-16	.00016	.00016	-3.84	-4.82	294
307.7	3.2	1.304E-15	5.872E-18	8.1E-5	8.1E-5	-3.84	-4.82	294
300	3.3	5.537E-16	2.151E-18	6.5E-5	6.5E-5	-3.84	-4.82	294
285.7	3.5	9.983E-17	2.888E-19	4.2E-5	4.2E-5	-3.84	-4.82	294

Key:

T = Temperature in Kelvin

K⁻¹ = Inverse Temperature * 1000 in 1/Kelvin

CvCuTi2 = Total Vacancy Concentration

n_Cu_v or n_Ti_v = Cu or Ti₂ Vacancy Concentration Fractionn_Cu_a or n_Ti_a = Cu or Ti₂ Antisite Defect Concentration FractionmuCu or muTi2 = Cu or Ti₂ Chemical PotentialNCu = Cu or Cu*2 = Ti₂ Number of lattice sites at a given Temperature (T)

Table 17. Vacancy Concentration of FeTi, NiTi, CuTi, & CuTi₂

Temp(K)	K ⁻¹	CvCuTi ₂	CvCuTi	CvFeTi	CvNiTi
10000	.1	.5436065413	.5065858619	.4007871513	.2218786602
5000	.2	.1632134099	.1299487611	.0868619735	.0286304315
3333.3	.3	.0502867013	.0337499548	.0203580644	.0041374068
2500	.4	.0157050543	.0088671528	.0050368411	.0006441605
2000	.5	.0049667039	.0023544524	.0012977370	.0001055932
1666.7	.6	.0015931990	.0006311847	.0003449970	1.790519E-5
1428.6	.7	.0005185351	.0001706591	.0000938990	3.101577E-6
1250	.8	.0001710892	4.648931E-5	2.599875E-5	5.443513E-7
1200	.833	.0001185558	3.018146E-5	1.699486E-5	3.053709E-7
1111.1	.9	5.714868E-5	1.274647E-5	7.287051E-6	9.630086E-8
1000	1	1.929607E-5	3.514274E-6	2.060060E-6	1.711839E-8
909.1	1.1	6.576084E-6	9.734784E-7	5.858714E-7	3.051736E-9
833.3	1.2	2.258967E-6	2.707338E-7	1.673087E-7	5.44982E-10
750	1.33	5.490644E-7	4.939816E-8	3.159793E-8	5.48906E-11
714.3	1.4	2.716983E-7	2.113923E-8	1.374903E-8	1.74272E-11
666.7	1.5	9.494356E-8	5.929085E-9	3.950536E-9	3.11853E-12
571.4	1.75	6.963697E-9	2.48986E-10	1.75429E-10	4.22771E-14
545.5	1.83	2.926309E-9	8.67145E-11	6.21618E-11	1.00820E-14
500	2	5.18962E-10	1.05413E-11	7.80877E-12	5.73400E-16
444.4	2.25	3.90646E-11	4.48752E-13	3.47911E-13	7.77566E-18
428.6	2.33	1.65196E-11	1.56836E-13	1.23350E-13	1.78124E-18
400	2.5	2.95910E-12	1.91788E-14	1.55065E-14	1.03795E-19
363.6	2.75	2.25032E-13	8.22104E-16	6.91224E-16	1.44926E-21
352.9	2.83	9.53972E-14	2.87874E-16	2.45091E-16	3.41426E-22
333.3	3	1.71555E-14	3.53173E-17	3.08140E-17	
307.7	3.25	1.30990E-15	1.52076E-18	1.44896E-18	
300	3.33	5.55843E-16	5.33225E-19	4.59591E-19	
285.7	3.5	1.00114E-16	6.47763E-20		

Key:

Temp = Temperature in Kelvin

K⁻¹ = Inverse Temperature * 1000 in 1/Kelvin

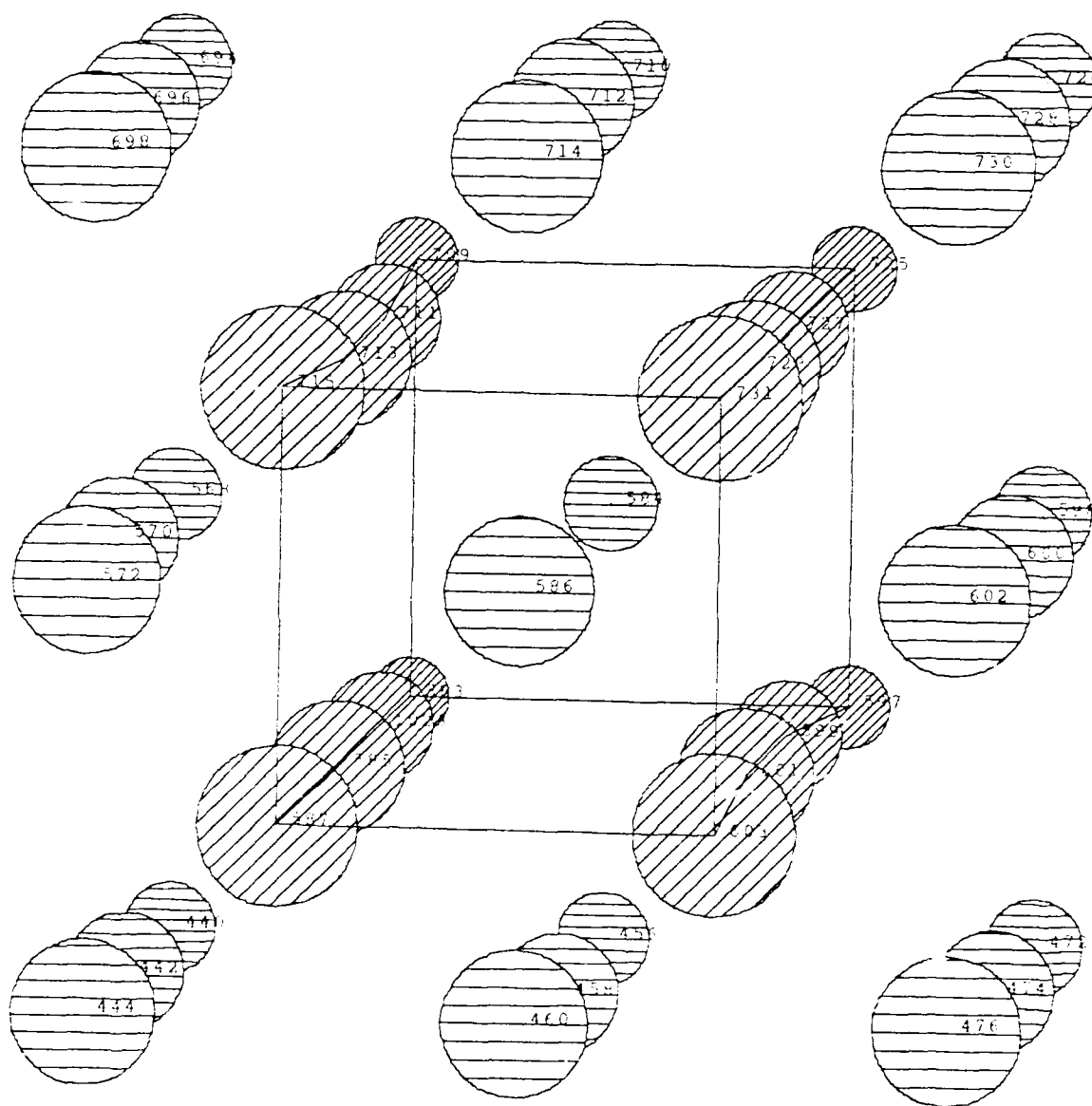
Table 18. Vacancy Formation Energy (Ef)

Temp(K)	T(K ⁻¹)	CuTi2(eV)	CuTi(eV)	FeTi(eV)	NiTi(eV)
10000	.1				
5000	.2	1.03681	1.17275	1.31769	1.76454
3333.33	.3	1.01454	1.16207	1.25024	1.66694
2500	.4	1.00285	1.15212	1.20358	1.60272
2000	.5	.99205	1.14300	1.16865	1.55832
1666.66	.6	.97980	1.13474	1.14166	1.52915
1428.57	.7	.96729	1.12738	1.12139	1.51078
1250	.8	.95551	1.12093	1.10662	1.49948
1200	.833333	.94826	1.11709	1.09907	1.49442
1111.11	.9	.94325	1.11448	1.09459	1.49173
1000	1	.93563	1.11057	1.08868	1.48850
909.091	1.1	.92763	1.10651	1.08354	1.48601
833.333	1.2	.92079	1.10309	1.07998	1.48452
750	1.33333	.91416	1.09979	1.07722	1.48353
714.286	1.4	.90938	1.09743	1.07561	1.48302
666.667	1.5	.90604	1.09578	1.07468	1.48276
571.429	1.75	.90054	1.09305	1.07351	1.48248
545.454	1.83333	.89652	1.09102	1.07285	1.48236
500	2	.89431	1.08986	1.07260	1.48232
444.444	2.25	.89159	1.08835	1.07236	1.48239*
428.571	2.33333	.89000	1.08739	1.07226	1.52392*
400	2.5	.88914	1.08680	1.07222	1.46977*
363.636	2.75	.88807	1.08597	1.07219	1.47231*
352.941	2.83333	.88744	1.08540	1.07217	1.49495*
333.333	3	.88710	1.08502	1.07217	
307.692	3.25	.88668	1.08486*	1.05377*	
300	3.33333	.88643	1.08245*	1.18740*	
285.714	3.5	.88630	1.08401*		

* These values are less accurate due to their having vacancy concentrations equal to or less than 1E-18, thus their calculation errors are about equal to the tolerance values of the TK Solver model calculation.

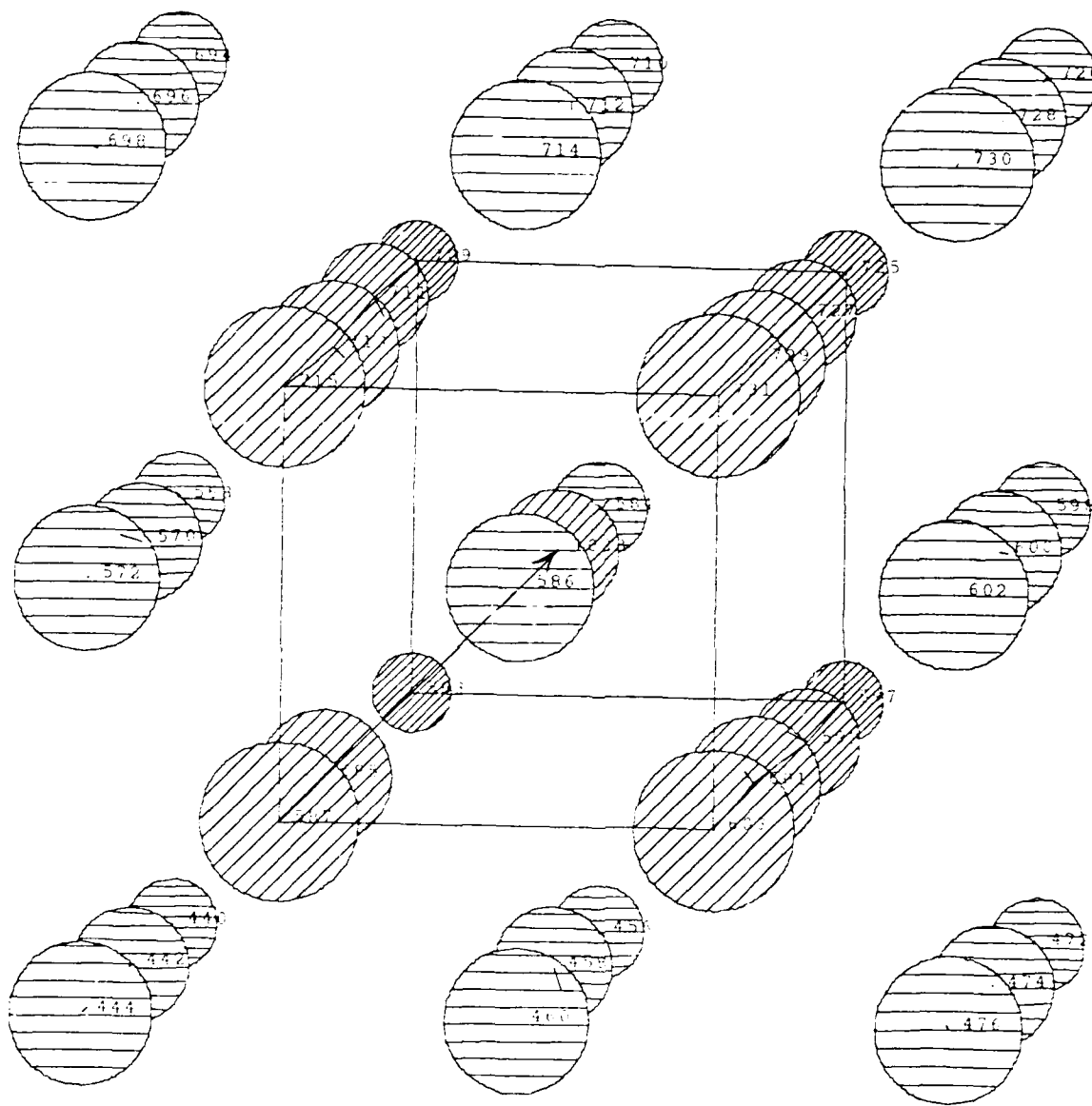
APPENDIX D: Stable Defect Configuration Plots

The following figures are output plots from the RUNDYN code for each of the most stable defect configurations plus example plots of vacancy and migration configurations. Figures 12 and 14 are minimized vacancy configurations, but are not the most stable defect configurations. The most stable configurations for these lattices are Figures 13 and 15 respectively. Figures 18 through 22 are examples of Fe vacancy migrations. The Ni vacancy migration plots were similar in all respects except the configuration in Figure 21 was stable for NiTi. The remaining Figures 23 through 38 are all of the most stable interstitial configurations for either NiTi or FeTi. In all cases the Ti atoms are symbolized with circles with horizontal lines and the Ni or Fe atoms are symbolized with circles with diagonal lines. Except where noted all of these figures have unit direction views of $x=1$, $y=0.1$, and $z=0.1$. All of the figures in this Appendix were reproduced from the AFIT mainframe system. The rest of this thesis was written using the Lotus software programs Manuscript release 2.1 and Freelance release 3.01.



Sun Sep 23 17:58:16 1990 : nitivacmin.res

Figure 12. NiTi Lattice with Ti Vacancy Minimized



Mon Sep 24 12:28:34 1990 - niti pin res

Figure 13. NiTi Lattice with Ti Vacancy Configuration
Trajectories from Figure 12

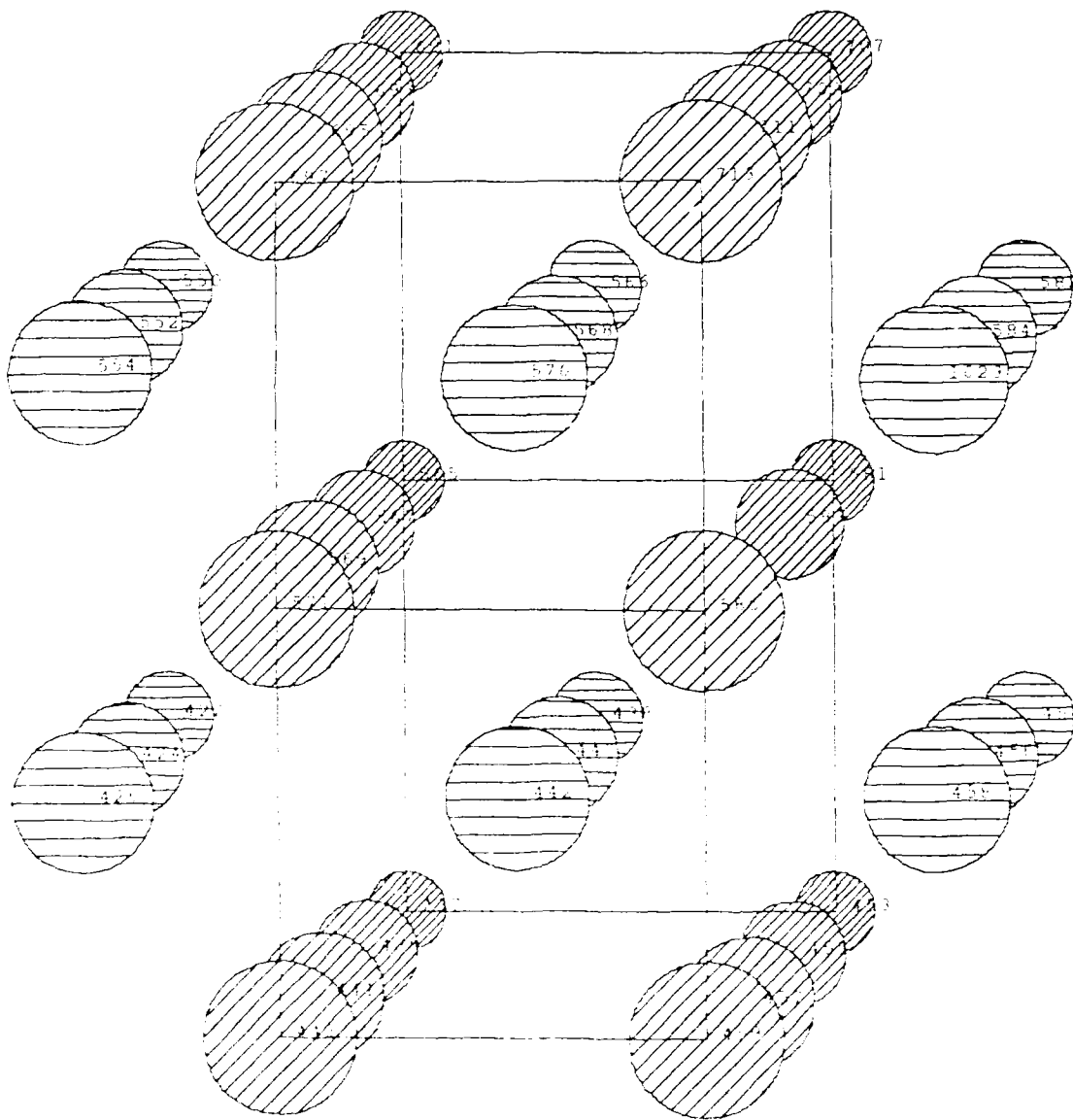
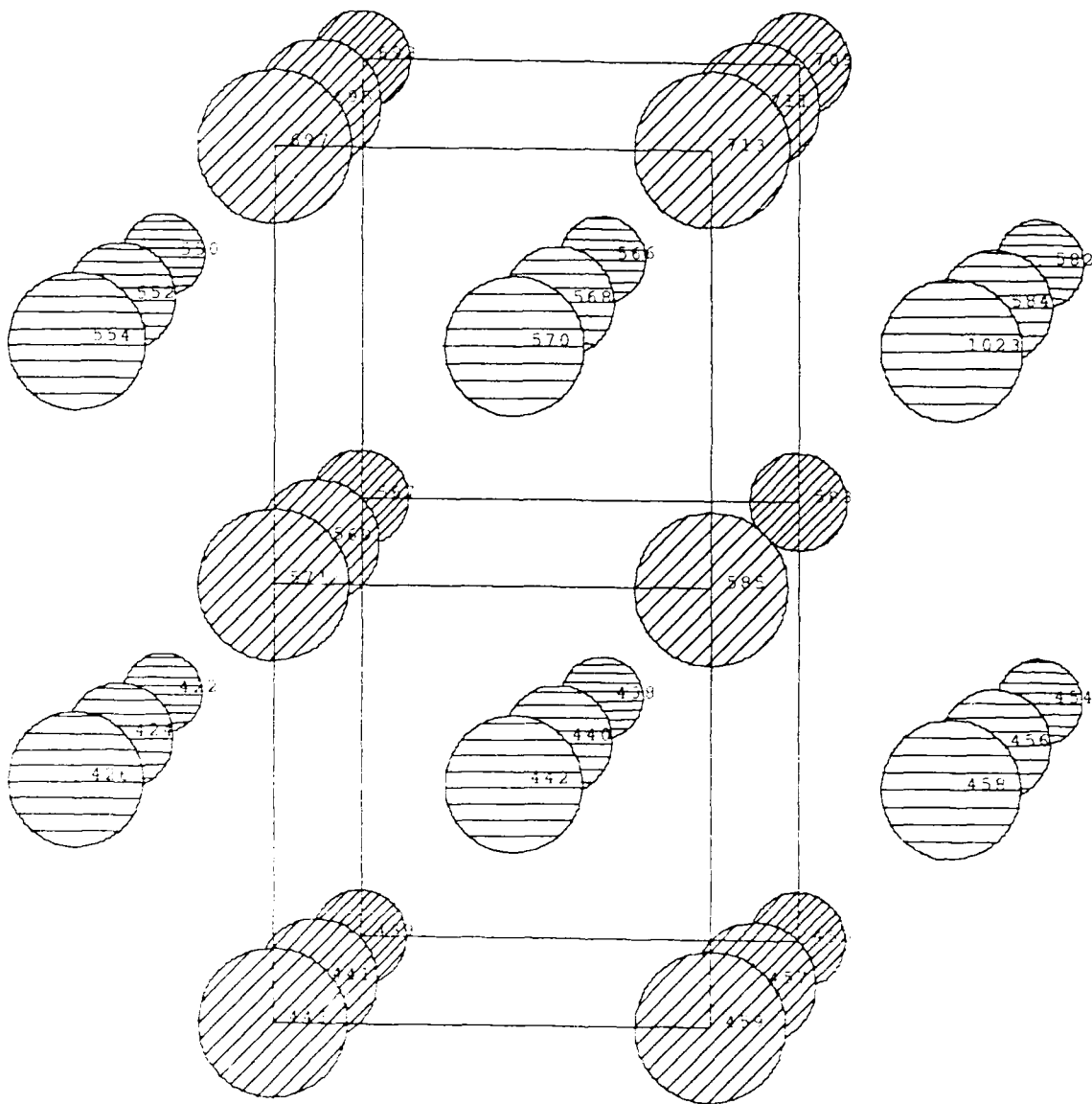


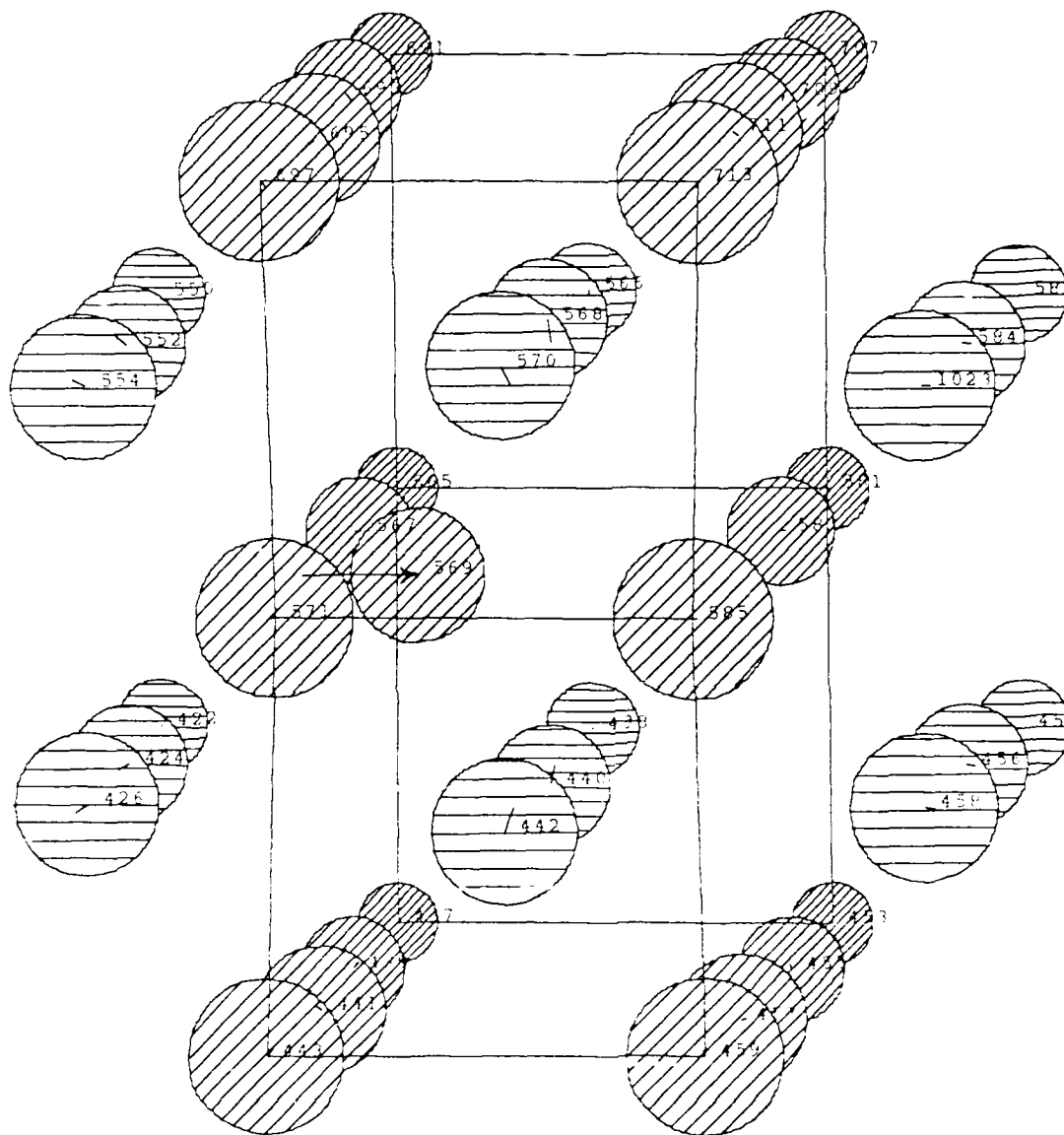
Figure 16. NiTi Lattice with Ni Vacancy Configuration

Figure 16. NiTi Lattice with Ni Vacancy Configuration



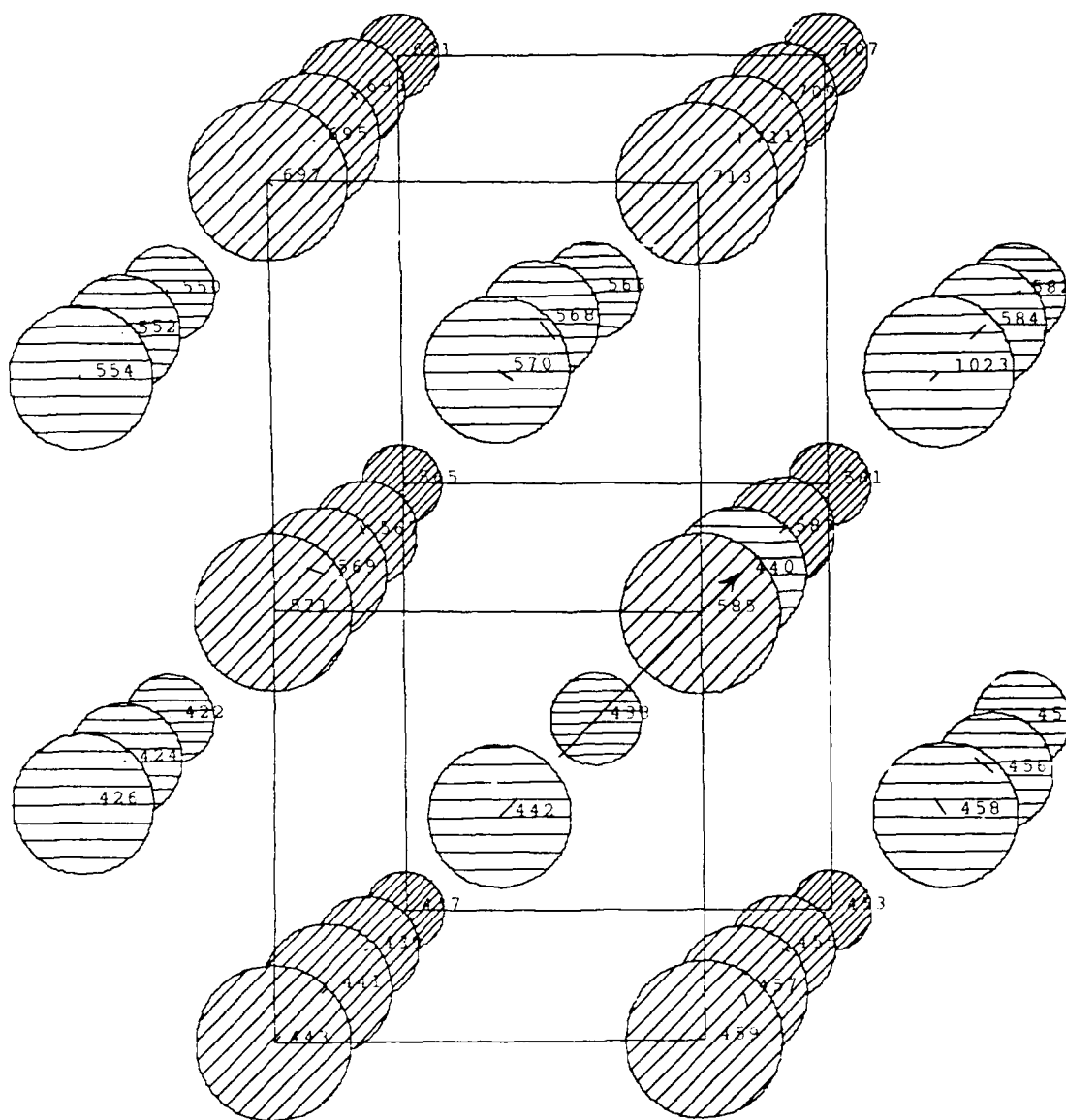
This Sep 1 10 42:21 1991 fevac.stt

Figure 17. FeTi Lattice with Fe Vacancy Configuration



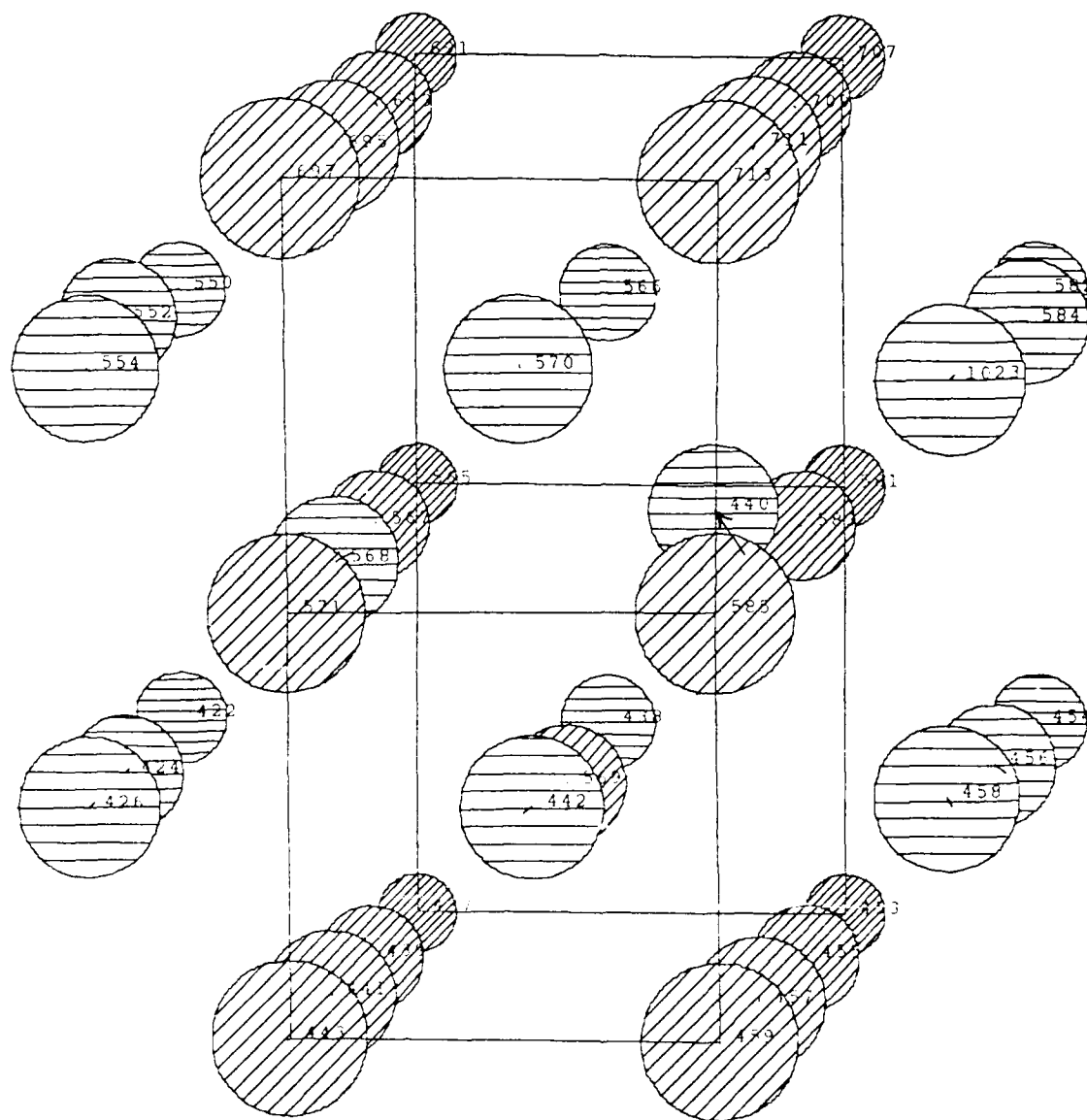
Fri Sep 14 15:23:04 1990 : fe569.-.50.res

Figure 18. FeTi Lattice with Fe Vacancy Direct Migration
Atom #569



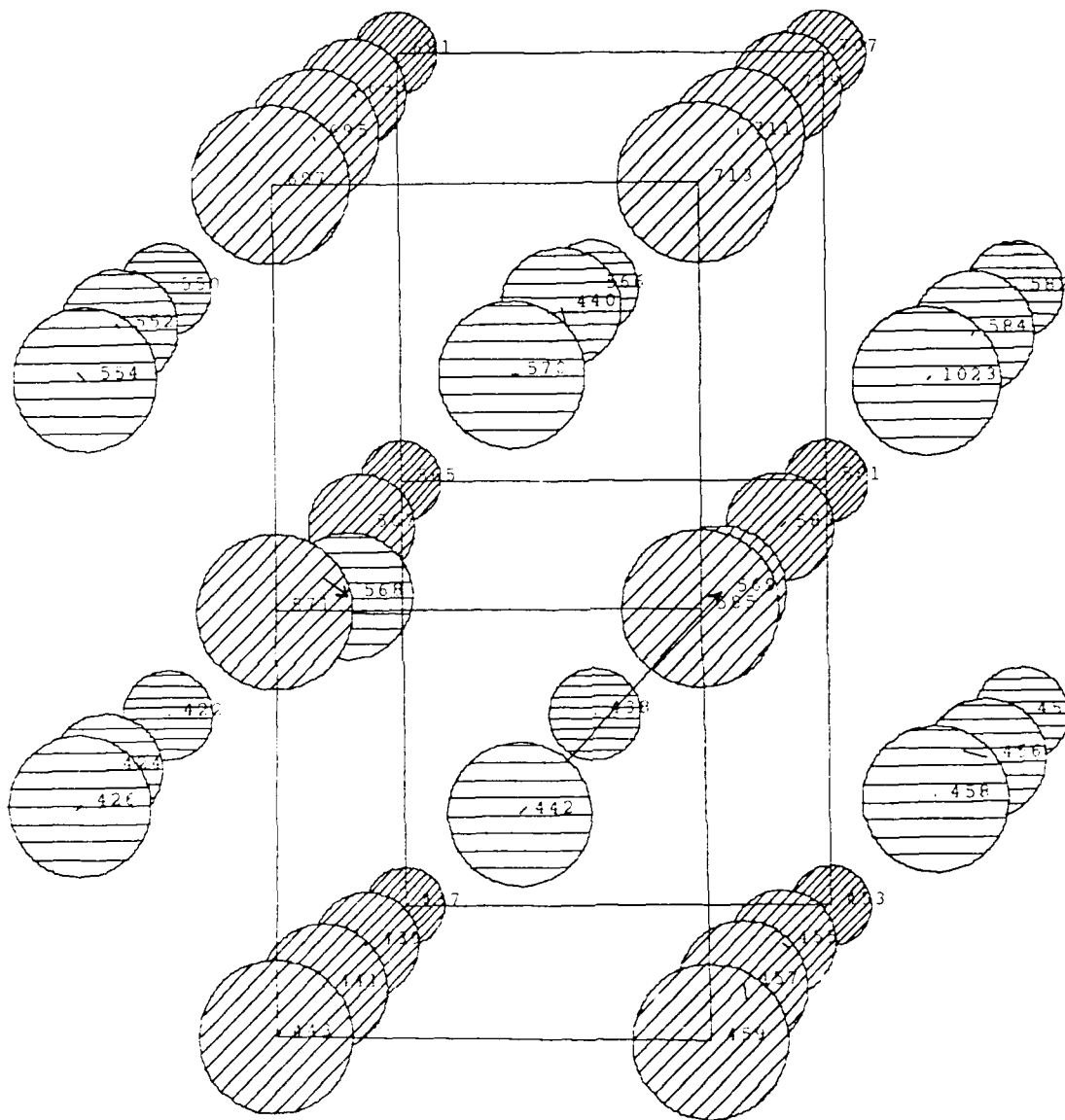
Fri Sep 14 23:02:30 1990 : ti440.+1.0.res

Figure 19. FeTi Lattice with Fe Vacancy Migration Sequence
#1 of Atom #440



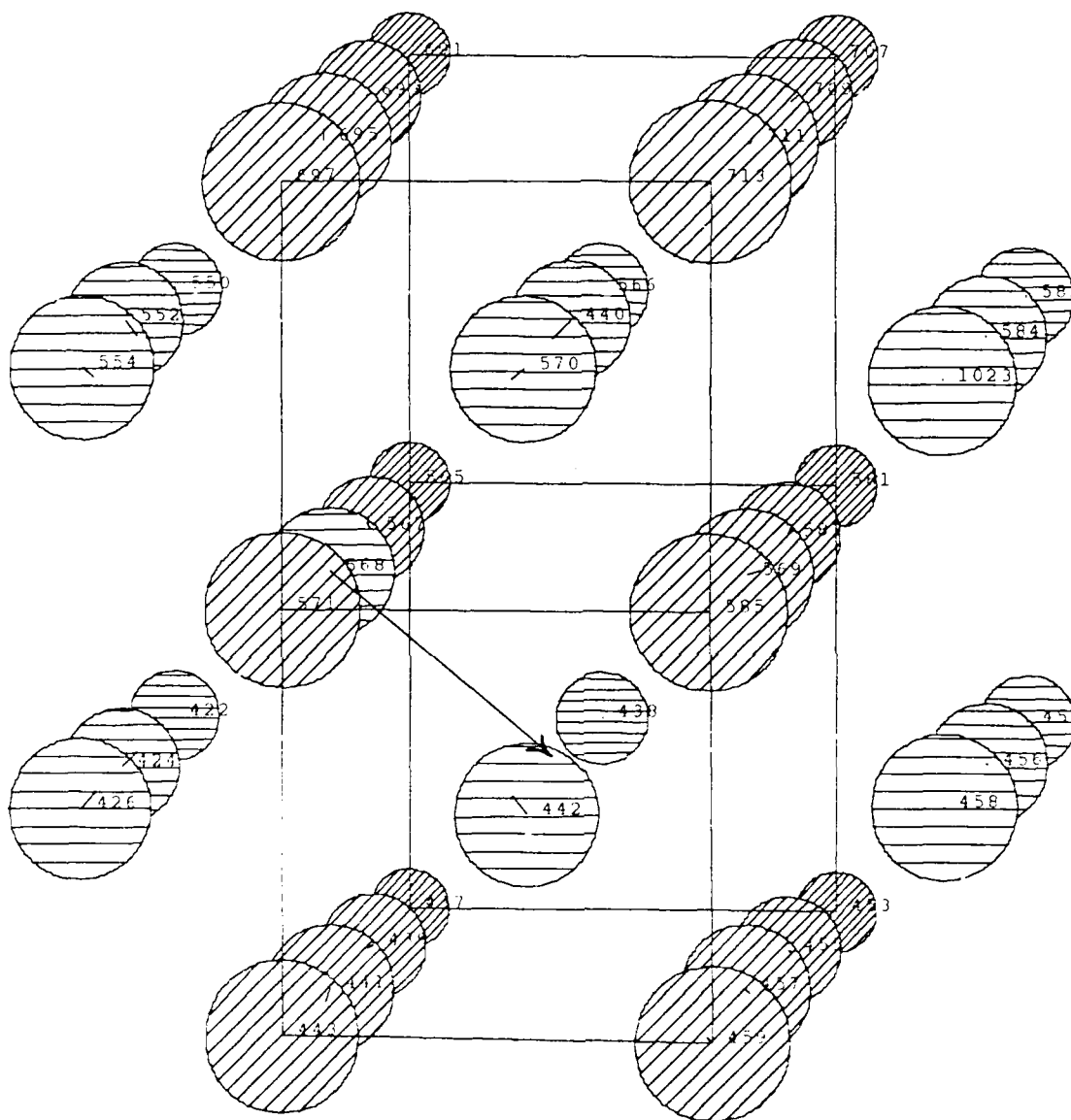
Sat Sep 15 23:40:19 1990 : ti440b.-.50.res

Figure 20. FeTi Lattice with Fe Vacancy Migration Sequence
#4 of Atom #440



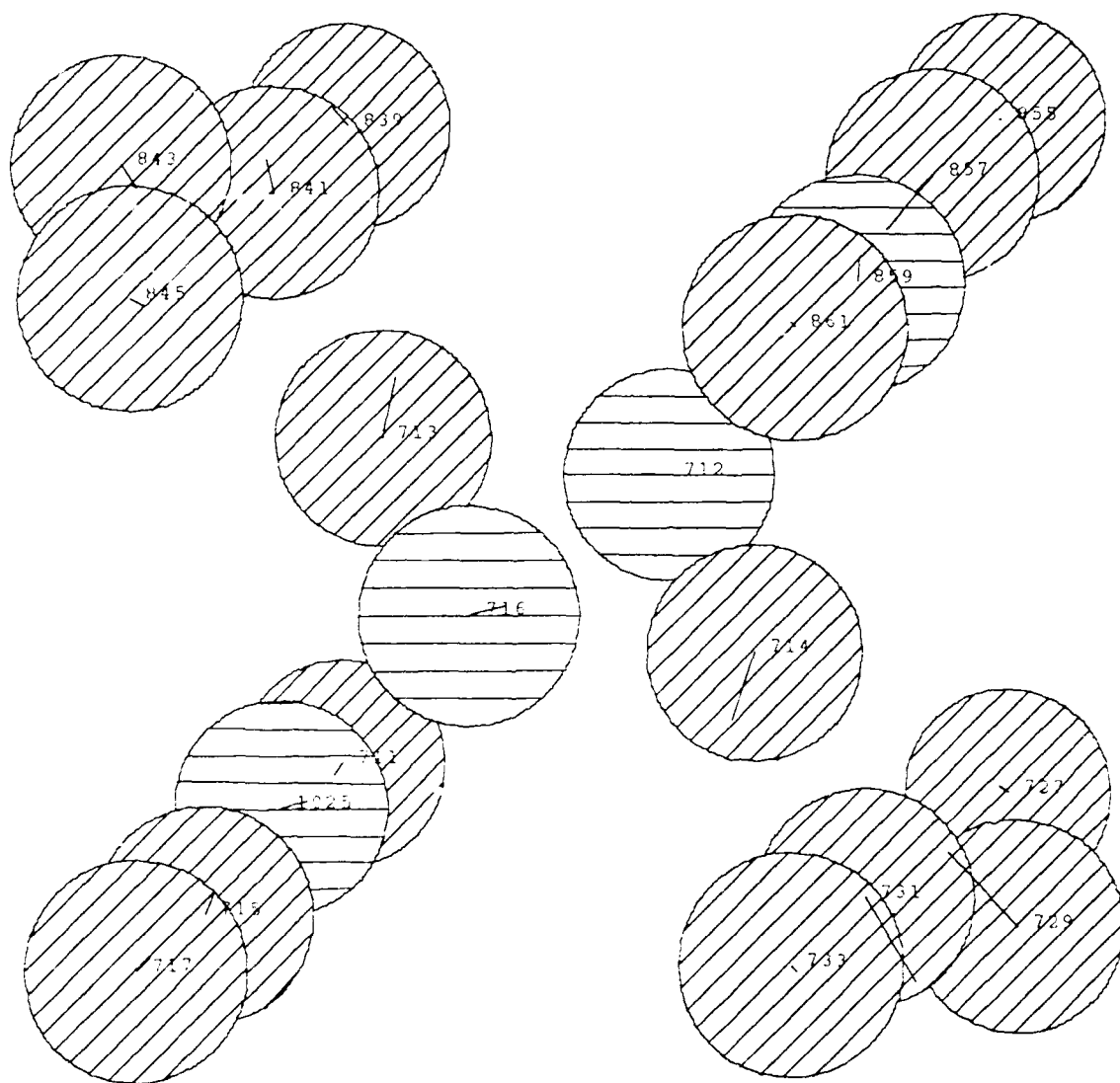
Sun Sep 16 22:09:51 1990 : fe569b.4.75.res

Figure 21. FeTi Lattice with Fe Vacancy Migration Sequence
 #5 of Atom #569 is Unstable with Atom #568 Also Moving



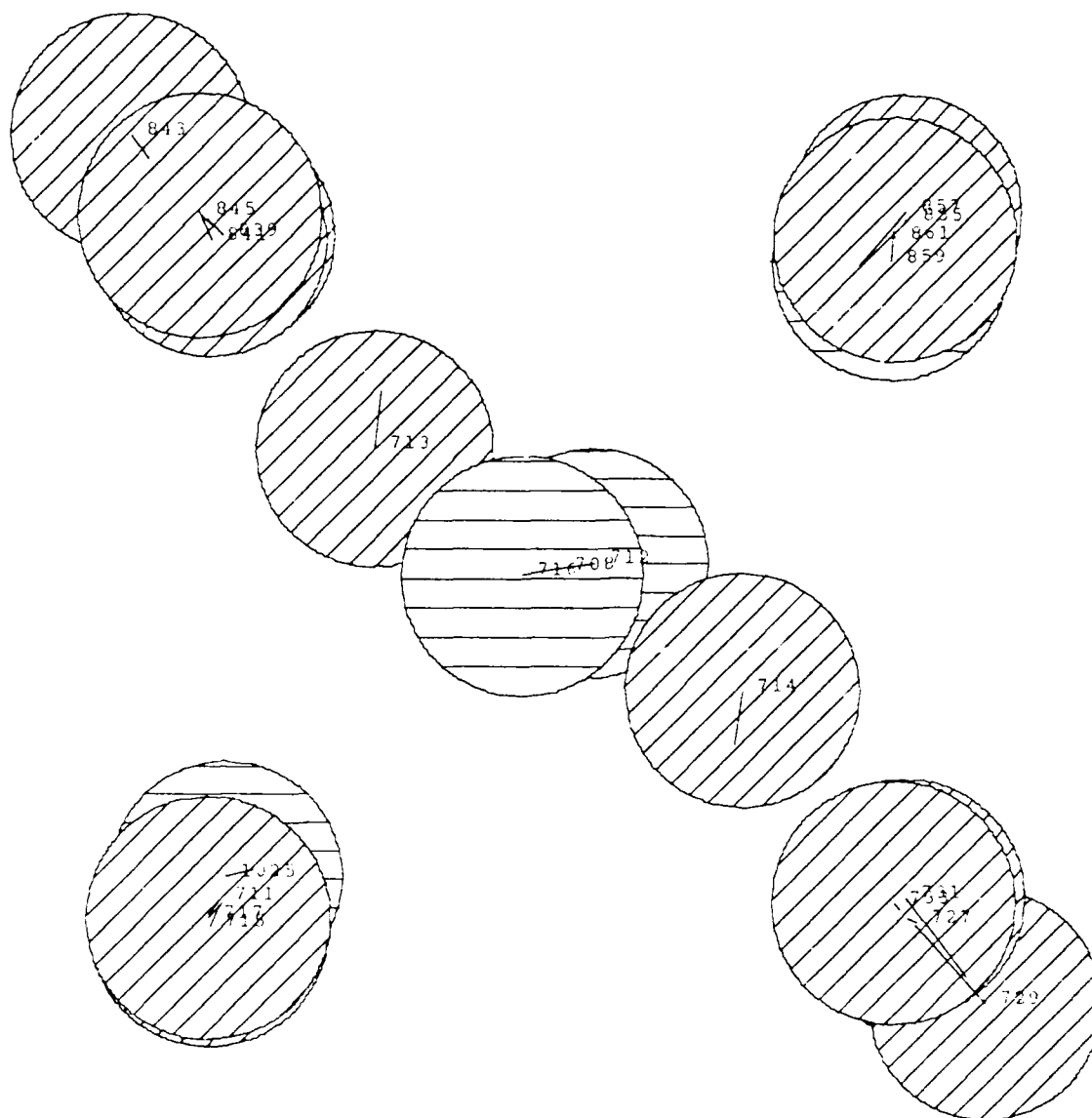
Thu Sep 20 12:06:34 1990 : ti568b.+1.0.res

Figure 22. FeTi Lattice with Fe Vacancy Migration Sequence
#6 of Atom #568



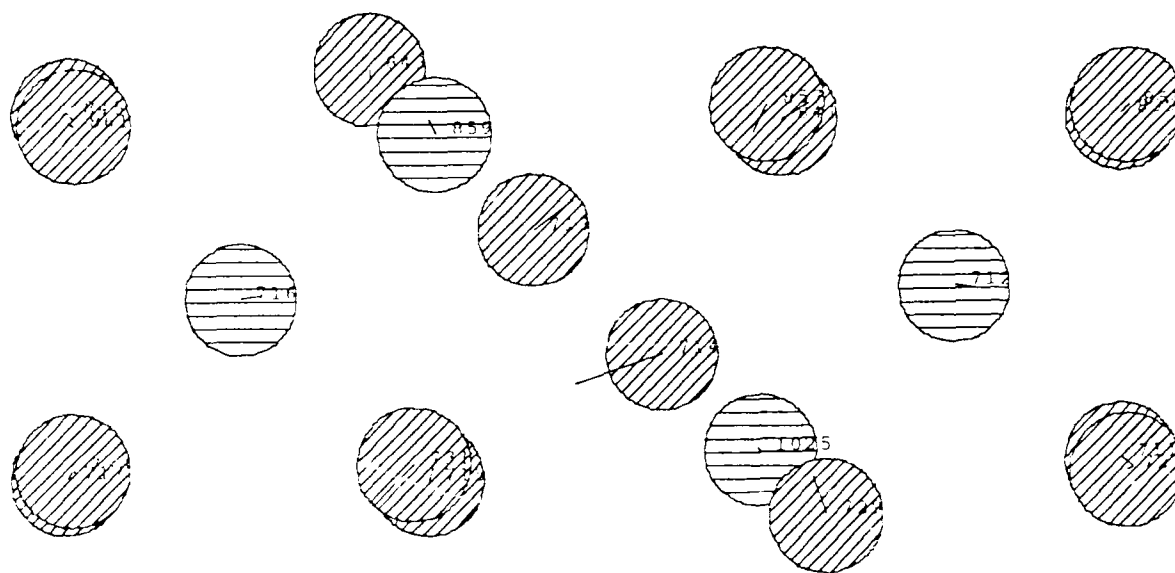
Mon Oct 15 14:11:16 1990 : nitl_intl.test4.res

Figure 23. NiTi Ti Interstitial Configuration, Trajectories from Figure 27



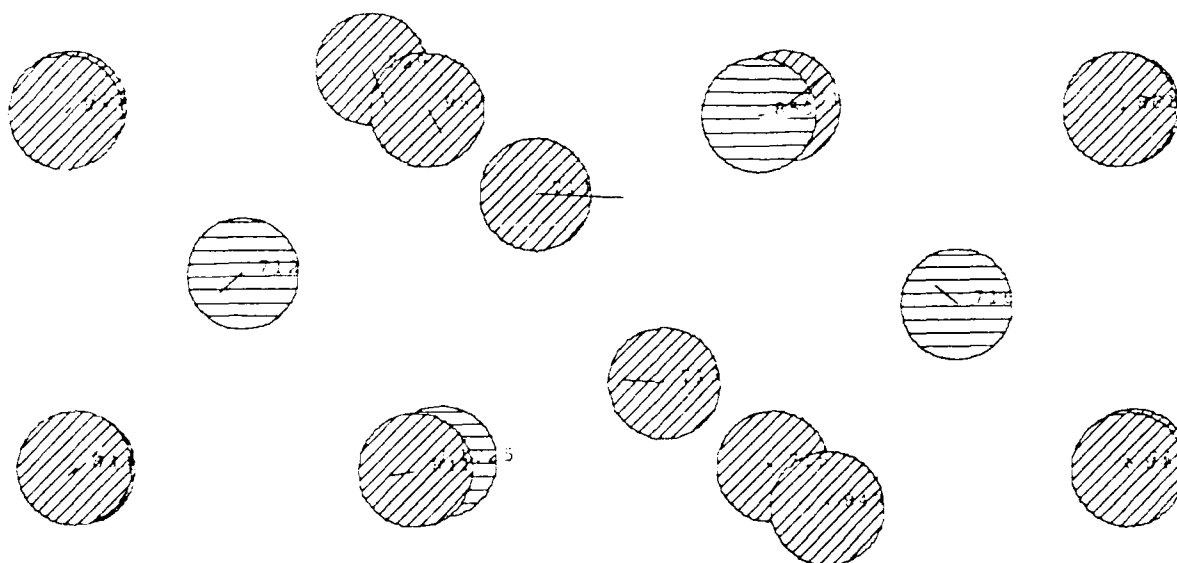
Thu Oct 11 20:22:41 1990 : niti_intl.test4.res

Figure 24. NiTi Ti Interstitial Configuration <100> View



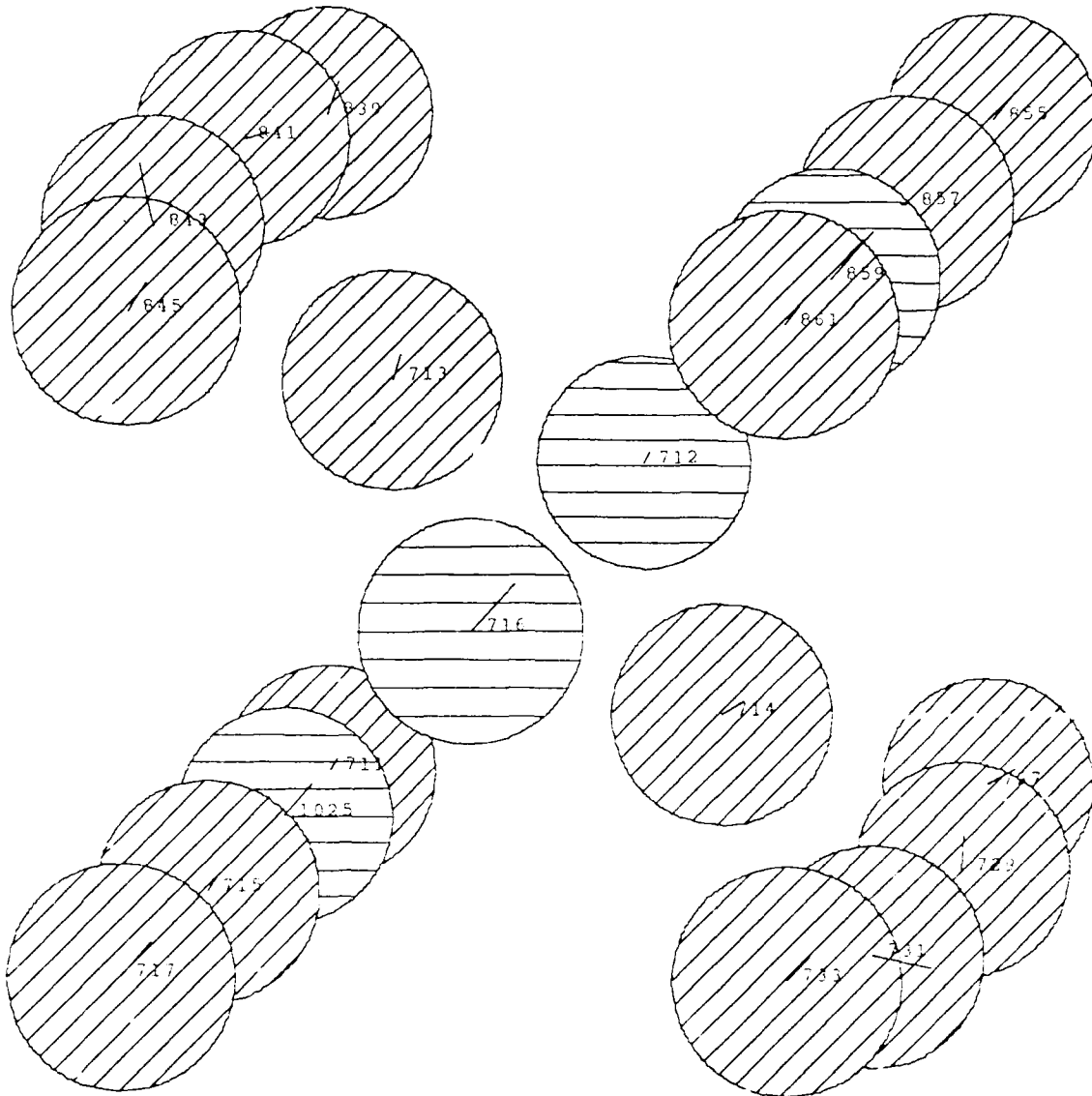
Mon Oct 15 14:15:00 1990 : niti_intl.test4.res

Figure 25. NiTi Ti Interstitial Configuration <010> View



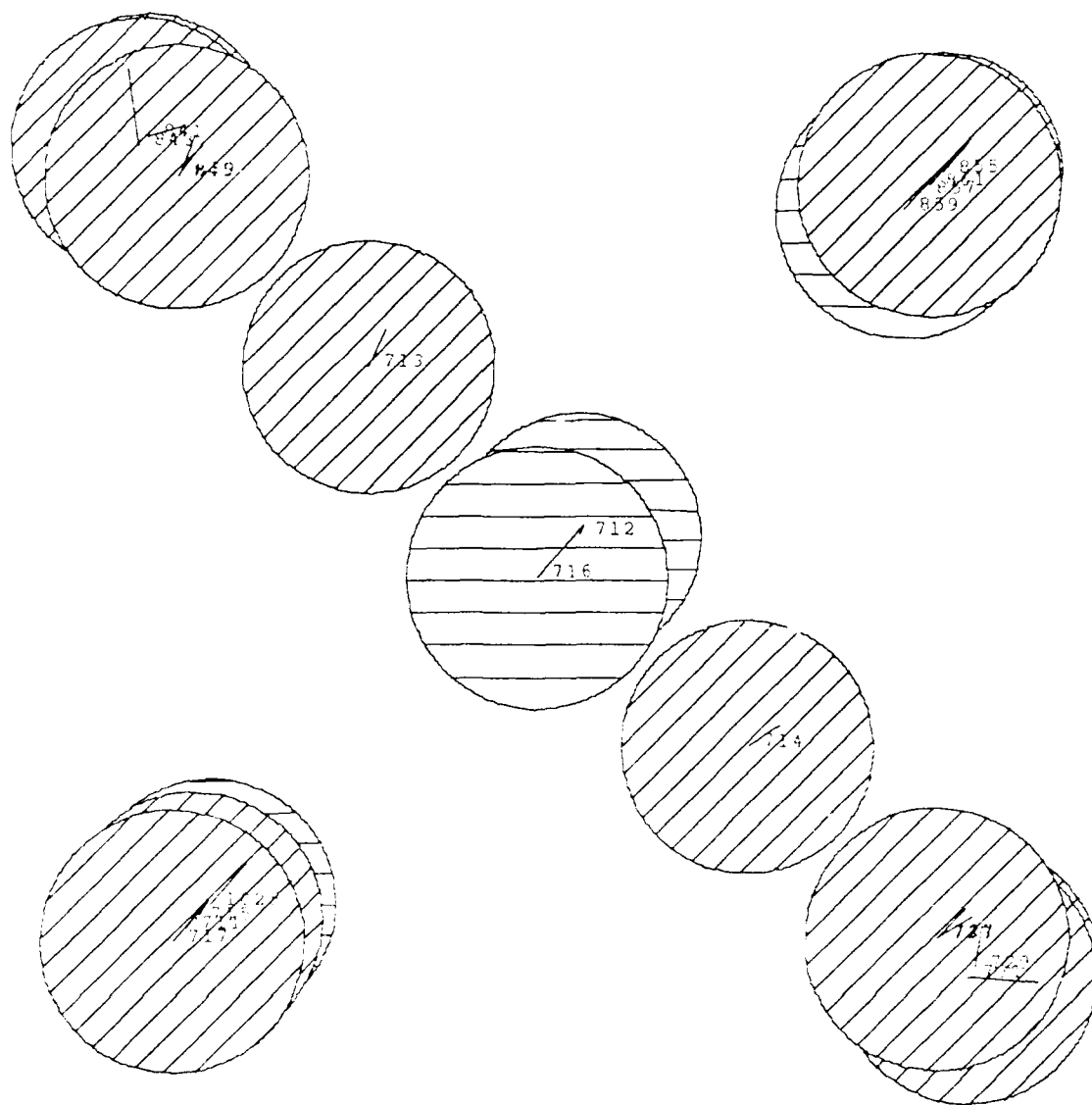
Mon Oct 15 14:05:54 1990 : niti_intl.test4.res

Figure 26. NiTi Ti Interstitial Configuration <001> View



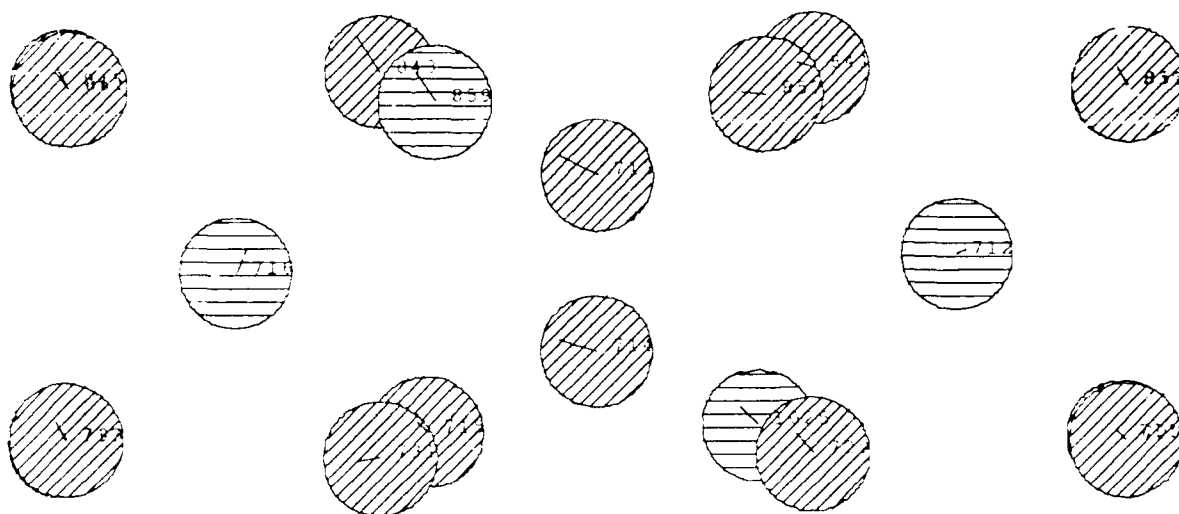
Mon Oct 15 13:39:55 1990 : feti_intl.test4.res2

Figure 27. FeTi Ti Interstitial Configuration



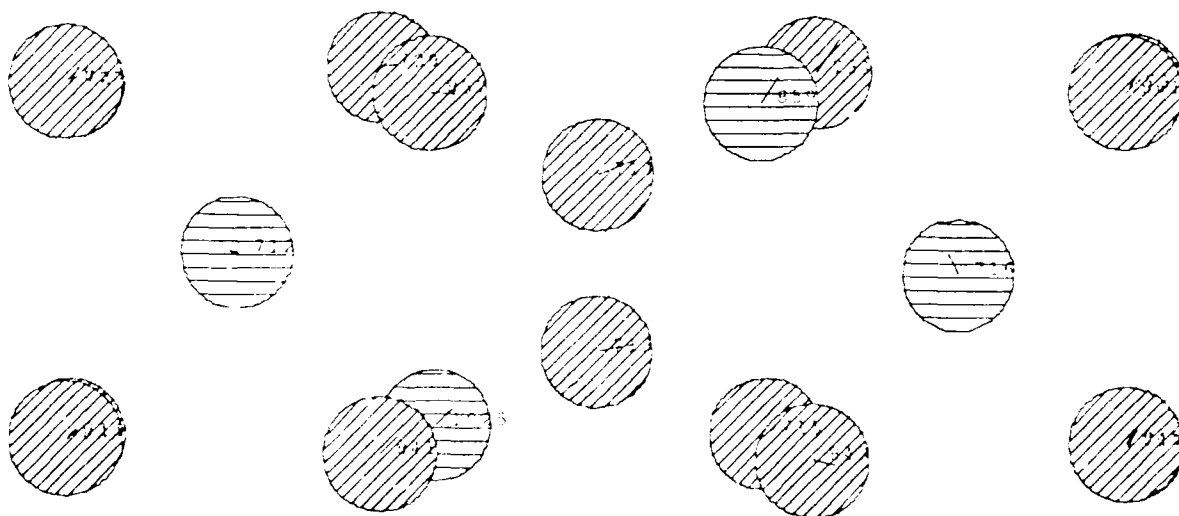
Mon Oct 15 13:43:40 1990 : feti_intl.test4.res2

Figure 28. FeTi Ti Interstitial Configuration <100> View



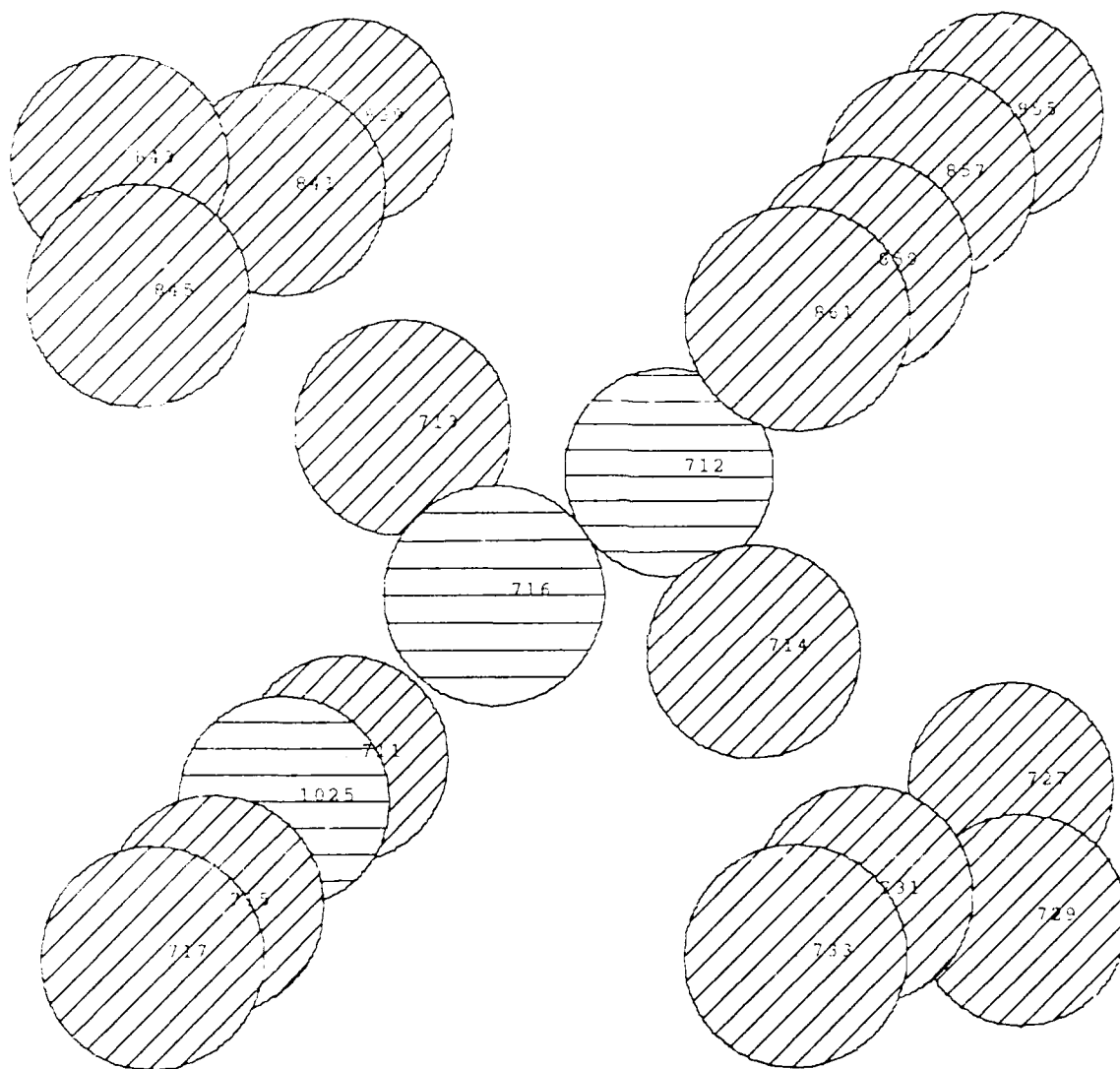
Mon Oct 15 11:50:48 1990 : feti_intl.test4.res2

Figure 29. FeTi Ti Interstitial Configuration <010> View



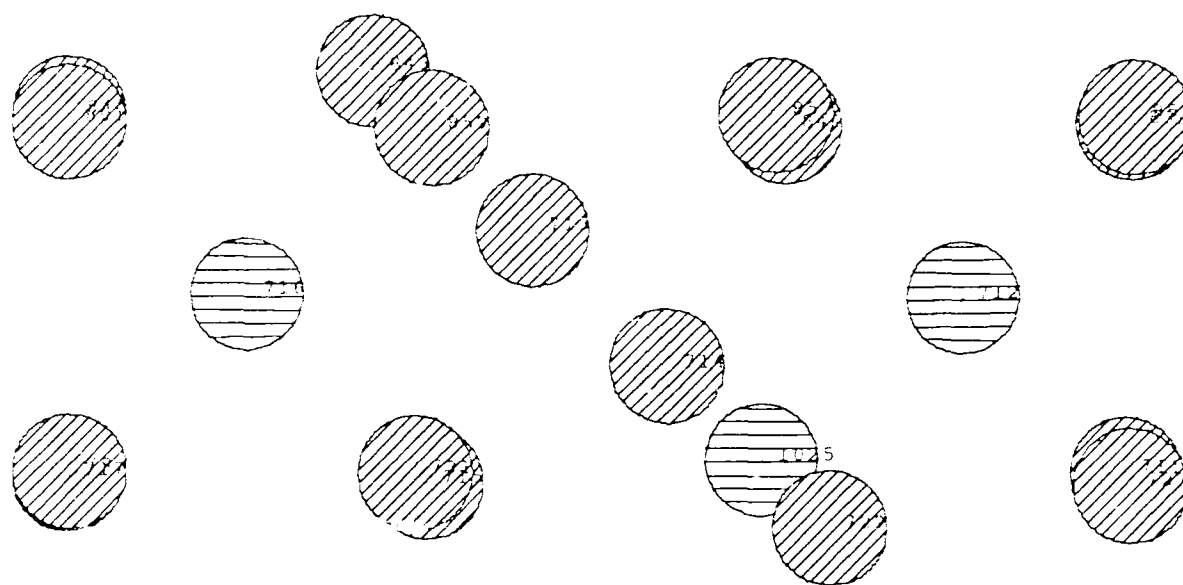
Mon Oct 15 13:59:03 1990 : feti_intl.test4.res2

Figure 30. FeTi Ti Interstitial Configuration <001> View



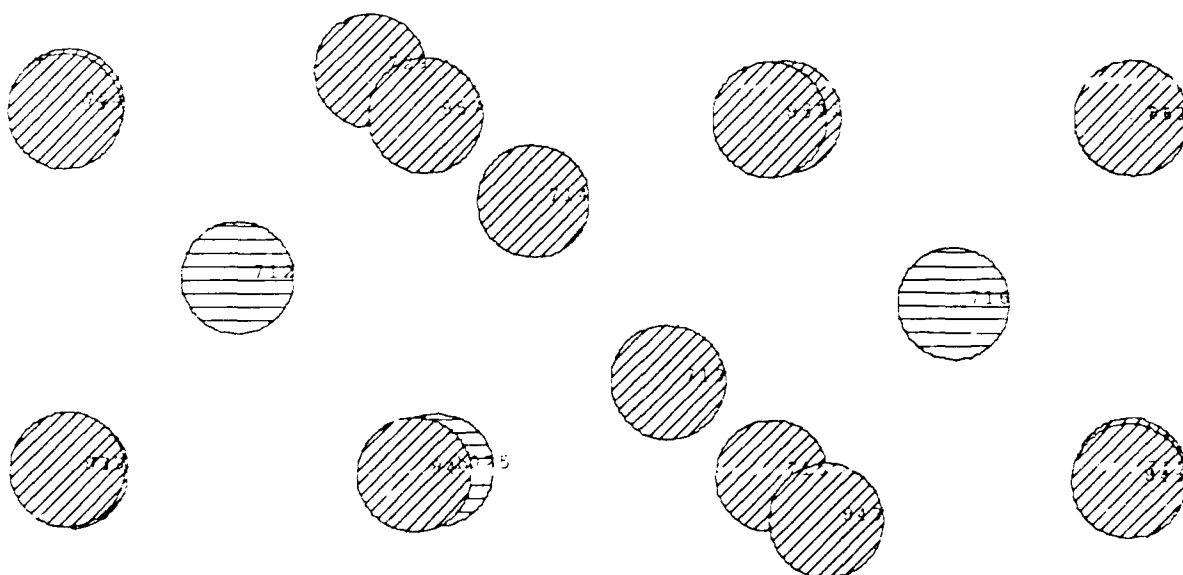
Tue Oct 16 00:23:05 1990 : ni_intl.test3.res

Figure 31. NiTi Ni Interstitial Configuration



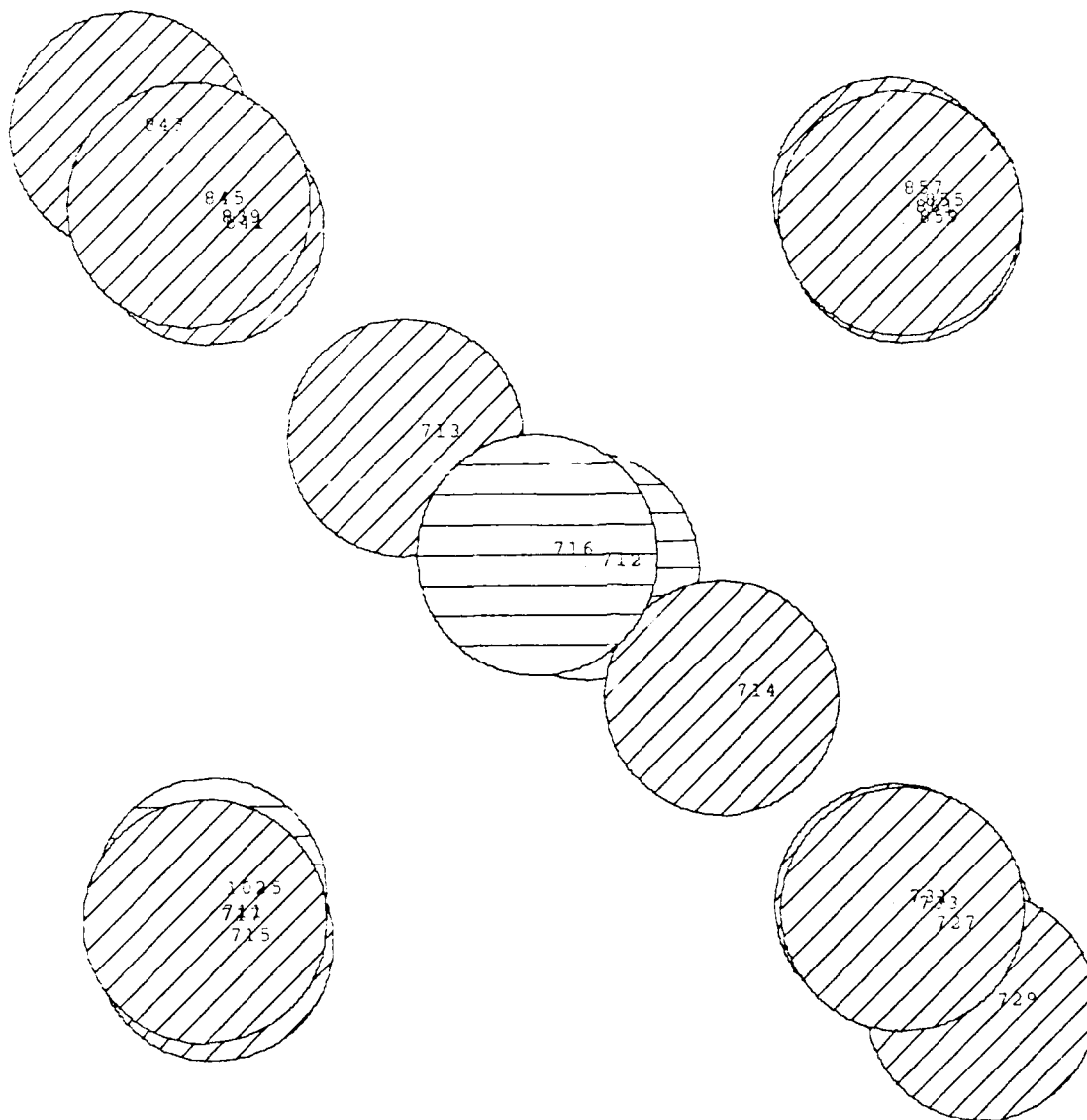
Tue Oct 16 00:25:53 1990 : ni_intl.test3.res

Figure 33. NiTi Ni Interstitial Configuration <010> View



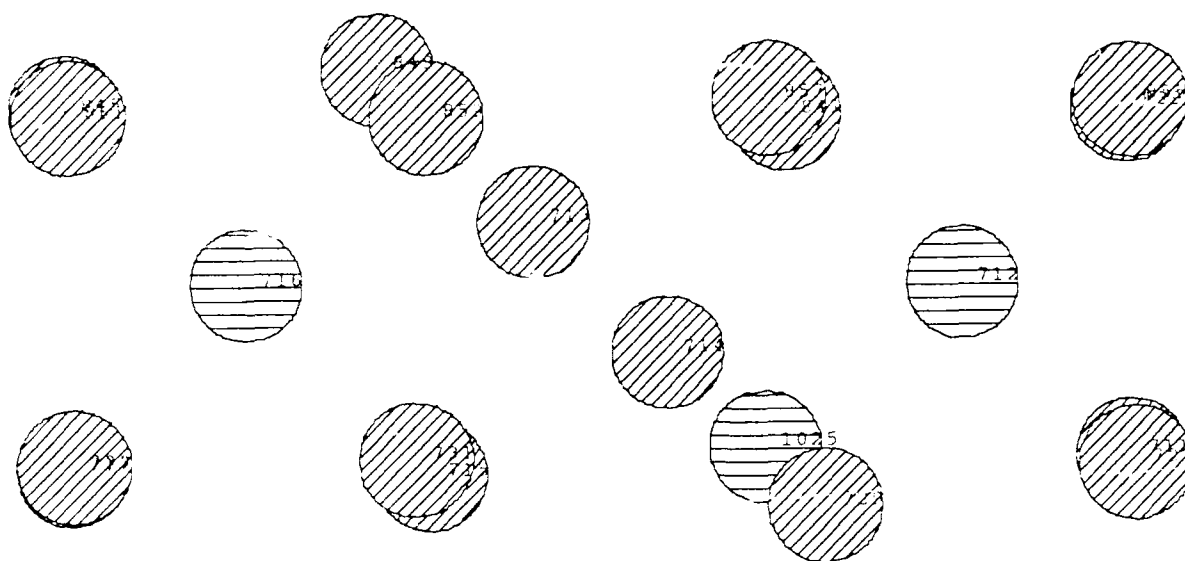
Tue Oct 16 00:26:40 1990 : ni_intl.test3.res

Figure 34. NiTi Ni Interstitial Configuration <001> View



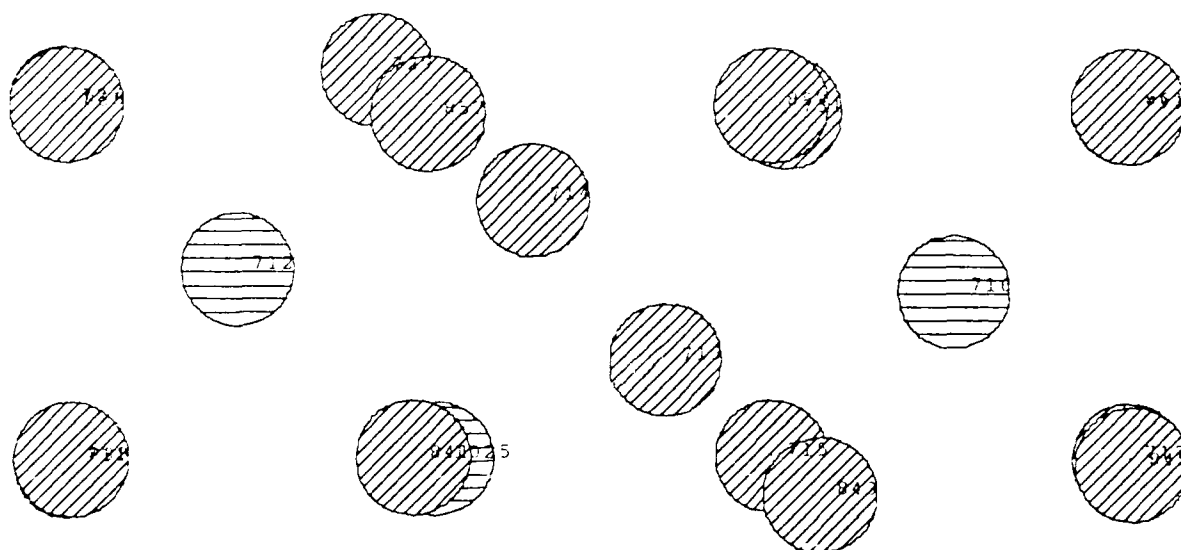
Tue Oct 16 00:12:54 1990 : fe_intl.test3.res

Figure 36. FeTi Ti Interstitial Configuration <100> View



Tue Oct 16 00:14:50 1990 : fe_intl.test3.res

Figure 37. FeTi Fe Interstitial Configuration <010> View



Tue Oct 16 00:18:52 1990 : fe_intl.test3.res

Figure 38. FeTi Fe Interstitial Configuration <001> View

Index

- Accuracy, vii, 10, 40, 98
- Amorphous
 - crystalline transition, 35
- Antisite
 - binding energy, 18
 - code input values, 48
 - defect properties, 14
 - energy, 35
 - formation energy, 12
 - pair energy, vii, 35
 - structure, 12
- Arrhenius plot, 29
- Atomistic simulation, 2, 4, 6, 23
 - techniques, 5
- B2-type Structure
 - FeTi, 7
 - NiTi, 7
- Binding energy, vii, 6, 17
- Boltzmann
 - constant, 23
- Boundary
 - code input conditions, 46
- Chemical disorder, 14, 35
- Critical temperature
 - Monte Carlo, 31
- Defect configurations
 - stable output plots, 69
- Dumbbell
 - Ni-Ni and Fe-Fe, 31
- DYNAMO code, vii, 5, 42
- Error
 - assessment, 10
 - TK Solver Plus, 61, 68
- FeTi
 - iron titanium, 3
 - melting temperature, 14
 - Ti interstitial, 32
- Fletcher-Powell
 - method, 42
 - minimization method, 5
 - minimizer, 48
- Formation energy
 - Fe antisite pair, 13
 - FeTi, NiTi, CuTi, CuTi₂, 68
 - interstitial, 38
 - Ni antisite, 13
 - vacancy, 24, 38, 60
- Frenkel pair
 - creation, 48
- Global minimum
 - configuration, 8
- Input file
 - RUNDYN code, 44
- Interatomic potential, 6
- Intermetallic compounds, 40
- Interstitial
 - configurations, 47
 - defect energy, viii
 - defect properties, 30
 - definition, 8
 - formation energy, 38
 - migration, 4
 - Ni and Fe, 34
 - stable configuration, 31
- Ion microscopy, 23
- Jumping atom, 43
- Lattice generation
 - code input, 46
- Lattice parameter
 - FeTi, 7
 - NiTi, 7
- Lotus 123
 - spreadsheet, 49
- Lotus software
 - Freelance, 69
 - Lotus 123, 49
 - Manuscript, 69
- Metastable
 - configuration, 8
- Migration
 - code input, 47
- Migration energy, 19
 - barrier, 15, 17, 21, 43
 - Ni or Fe atoms, 15
- Molecular dynamics, 5
- Molecular statics, 5
- Monte Carlo, 8
 - code input, 48
 - critical temperature, 30
 - technique, 5, 8, 30

NiTi
 melting temperature, 14
 nickel titanium, 3
 Ti interstitial, 32

 Output file, 45
 Output plots, 69

 Perfect lattice
 structure, 11
 system energy, 11
 Point defect
 definition, 1
 Potential energy, 5
 code input, 45

 Quenching
 metal, 23

 Reaction coordinate, 43
 Restart file, 45
 RUNDYN code, 5, 9
 description, 42

 Significant digits, 10, 49
 Simulated annealing, 5, 8, 30
 Softlink, 44
 Source code, 44
 Split-interstitial, viii, 37
 Cu-Cu, 39
 Ni-Ni dumbbell, 31
 Ni-Ni or Fe-Fe, 41
 Structure
 FeTi, 7
 NiTi, 7

 Ti Interstitial
 FeTi configuration, 32
 NiTi configuration, 32
 Ti Vacancy
 configuration, 16
 energy, 15
 TK Solver Plus
 iterative solver, 61
 software, 27
 software code, 56
 Tolerance, 10
 RUNDYN code, 48, 49
 TK Solver Plus, 61, 62, 68
 Transition
 crystalline-to-amorphous, 35

 Vacancy
 concentration, 23
 concentrations, 67
 configurations, 35
 CuTi concentration, 65
 CuTi2 concentration, 66
 defect energy, vii
 defect properties, 19
 definition, 8
 FeTi concentration, 64
 formation energy, 6, 36, 60, 86
 migration, vii, 36
 migration energy, 22
 migration sequence, 19
 Ni or Fe, 18
 NiTi concentration, 63
 Ti vacancy, 15

Bibliography

- Agullo-Lopez, F., C. R. A. Catlow, and P. D. Townsend. Point Defects in Materials. Academic Press, Harcourt Brace Jovanovich, Publishers, London, (1988).
- Crawford Jr., James H. and Lawrence M. Slifkin. Point Defects In Solids, Vol 1 General and Ionic Crystals. Plenum Press, New York-London, (1972).
- Foiles, S. M. and M. S. Daw. "Application of the embedded atom method to Ni₃Al," Journal of Material Research, 2: 5-15 (Jan/Feb 1987).
- Ghatak, A. K. and L. S. Kothari. An Introduction to Lattice Dynamics. Addison-Wesley Publishing Company, London, (1972).
- Haile, J. M. A Primer on the Computer Simulation of Atomic Fluids by Molecular Dynamics. Clemson University, Clemson, South Carolina, (November 1980).
- Lutton, Russell T., Michael J. Sabochick and Nghi Q. Lam. "Calculation of Defect Properties of NiTi and FeTi," Presented at the Material Research Society Fall Meeting, Symposium K, Defects in Materials, Boston MA, (November 26-30 1990).
- McQuillan, A. D. and M. K. McQuillan. Titanium. Academic Press Inc., Publishers, New York, (1956).
- Newkirk, J. B. and J. H. Wernick. Direct Observation of Imperfections in Crystals. Interscience Publishers, New York, (1962). Sabochick, Michael J. "Basic Primer on atomistic simulation," unpublished, (1990).
- Sabochick, Michael J. Personal conversation, (December 1990).

Sabochick, Michael J. and Nghi Q. Lam. "Atomistic Simulation of Radiation-Induced Amorphization of the B2 Ordered Intermetallic Compound NiTi," Presented at the Material Research Society Fall Meeting, Symposium K, Defects in Materials, Boston MA, (November 26-30 1990).

Shoemaker, J. R., R. T. Lutton, D. Wesley, W. R. Wharton, M. L. Oehrli, M. S. Herte, and M. J. Sabochick. "Point Defect Study of CuTi and CuTi₂," to be published in Journal of Material Research, (October 1990).

TK Solver Plus Version 1.1. Universal Technical Systems, Inc., Rockford, Illinois.

Vita

Captain Russell Thomas Lutton was born in Portsmouth, Virginia on 17 July 1952. He received his Bachelor of Science in Physics from Old Dominion University in Norfolk, Virginia in May 1974. Continuing his education at the Institute of Oceanography in Norfolk, Virginia he received a Master of Science in Physical Oceanography in August 1979.

Captain Lutton was commissioned from Officer Training School on 4 February 1981. His first assignment was to the Air Force Weapons Laboratory (AFWL), Nuclear Technology Engineering Division (NTE) as a Computational Physicist and Project Officer. As the NTE hard Mobile Launcher (HML) small ICBM program manager, he was responsible for budget and construction of the 20 ft diameter 825 ft long nuclear simulation shocktube. He also predicted and analyzed shockwave loading using the "HULL" hydrodynamic computer code.

In May 1985, he was name requested by the Defense Nuclear Agency (DNA) to serve as Technical Director for their high explosive nuclear simulation events. He was awarded the Defense Meritorious Service Medal for his direction of the MISTY PICTURE 8 kiloton nuclear simulation event detonated in May 1987. After directing the MISERS GOLD 4 kT event detonated in June 1989, he was assigned to the School of Engineering, Air Force Institute of Technology in August 1989.

[REDACTED]

[REDACTED]

REPORT DOCUMENTATION PAGE

Form Approved
OMB No. 0704-0188

Public reporting burden for this collection of information is estimated to average 1 hour per response, including the time for reviewing instructions, searching existing data sources, gathering and maintaining the data needed, and completing and reviewing the collection of information. Send comments regarding this burden estimate or any other aspect of this collection of information, including suggestions for reducing this burden, to Washington Headquarters Services, Directorate for Information Operations and Reports, 1215 Jefferson Davis Highway, Suite 1204, Arlington, VA 22202-4302, and to the Office of Management and Budget, Paperwork Reduction Project (0704-0188), Washington, DC 20503.

1. AGENCY USE ONLY (Leave blank)		2. REPORT DATE March 1991		REPORT TYPE AND DATES COVERED Master's Thesis	
4. TITLE AND SUBTITLE CALCULATED POINT DEFECT PROPERTIES OF THE INTERMETALLIC COMPOUNDS NICKEL TITANIUM (NiTi) AND IRON TITANIUM (FeTi)				5. FUNDING NUMBERS	
6. AUTHOR(S) Russell T. Lutton, Captain, USAF					
7. PERFORMING ORGANIZATION NAME(S) AND ADDRESS(ES) Air Force Institute of Technology Wright-Patterson AFB, Ohio 45433-6583				8. PERFORMING ORGANIZATION REPORT NUMBER AFIT/GNE/ENP/91M-5	
9. SPONSORING MONITORING AGENCY NAME(S) AND ADDRESS(ES)				10. SPONSORING MONITORING AGENCY REPORT NUMBER	
11. SUPPLEMENTARY NOTES					
12a. DISTRIBUTION AVAILABILITY STATEMENT Approved for public release; distribution unlimited <i>nickel titanium and iron titanium.</i>				12b. DISTRIBUTION CODE <i>migration of a</i>	
13. ABSTRACT (Maximum 200 words) Atomistic simulation with a modified version of the DYNAMO code was used to calculate the point defect properties of the intermetallic compounds NiTi and FeTi. The calculated energies are believed to be experimentally accurate to within +/- 0.1 eV. Vacant Ni or Fe lattice sites were preferred and had energies of 3.356 eV for NiTi and 5.899 eV for FeTi. Removing a Ti atom resulted in a neighboring antisite defect caused by a migrating Ni or Fe atom into the vacant Ti site. These configurations had energies of 7.024 eV for NiTi and 6.336 eV for FeTi. The calculated vacancy defect formation energies were 1.48 eV for NiTi and 1.07 eV for FeTi. The interstitial defect configurations consisted of Ni-Ni or Fe-Fe split-interstitial dumbbells centered on a Ti site with one or two adjacent Ti antisite defects. Ti interstitials resulted in two adjacent Ti antisite defects with a <011> Fe-Fe dumbbell or a <111> Ni-Ni dumbbell. These Ti interstitial energies were -2.395 eV for NiTi and -1.558 eV for FeTi. Ni or Fe interstitials both resulted in an adjacent Ti antisite defect with Ni-Ni or Fe-Fe <111> oriented dumbbells. The Ni or Fe interstitial energies were -2.602 eV for NiTi and -1.945 eV for FeTi. <i>interstitial</i>					
14. SUBJECT TERMS Point Defects, Vacancy Defects, Interstitial Defects, Nickel Alloys, Iron Alloys, Titanium Alloys, Crystal Defects, DYNAMO Code, NiTi, FeTi, Point Defect Properties				15. NUMBER OF PAGES 107	
				16. PRICE CODE	
17. SECURITY CLASSIFICATION OF REPORT Unclassified	18. SECURITY CLASSIFICATION OF THIS PAGE Unclassified	19. SECURITY CLASSIFICATION OF ABSTRACT Unclassified	20. LIMITATION OF ABSTRACT UL		

98